

1 **Induced systemic resistance impacts the phyllosphere microbiome through plant-  
2 microbe-microbe interactions**

3  
4 Anna Sommer<sup>1</sup>, Marion Wenig<sup>1</sup>, Claudia Knappe<sup>1</sup>, Susanne Kublik<sup>2</sup>, Bärbel Fösel<sup>2</sup>, Michael  
5 Schloter<sup>2</sup>, and A. Corina Vlot<sup>1,\*</sup>

6  
7 <sup>1</sup>Helmholtz Zentrum Muenchen, Department of Environmental Science, Institute of  
8 Biochemical Plant Pathology, Ingolstaedter Landstr. 1, 85764 Neuherberg, Germany;

9 <sup>2</sup>Helmholtz Zentrum Muenchen, Department of Comparative Microbiome Analysis,  
10 Ingolstaedter Landstr. 1, 85764 Neuherberg, Germany

11  
12 \*Author for correspondence: corina.vlot@helmholtz-muenchen.de (+49-89-31873985)

13  
14 Funding: This work was funded by the DFG as part of priority program SPP 2125 (to MS and  
15 ACV).

16  
17 **Abstract**

18 Both above- and below-ground parts of plants are constantly confronted with microbes, which  
19 are main drivers for the development of plant-microbe interactions. Plant growth-promoting  
20 rhizobacteria enhance the immunity of above-ground tissues, which is known as induced  
21 systemic resistance (ISR). We show here that ISR also influences the leaf microbiome. We  
22 compared ISR triggered by the model strain *Pseudomonas simiae* WCS417r (WCS417) to that  
23 triggered by *Bacillus thuringiensis israelensis* (*Bti*) in *Arabidopsis thaliana*. In contrast to earlier  
24 findings, immunity elicited by both strains depended on salicylic acid. Both strains further relied  
25 on MYC2 for signal transduction in the plant, while WCS417-elicited ISR additionally depended  
26 on SAR-associated metabolites, including pipecolic acid. A metabarcoding approach applied  
27 to the leaf microbiome revealed a significant ISR-associated enrichment of amplicon sequence  
28 variants with predicted plant growth-promoting properties. WCS417 caused a particularly  
29 dramatic shift in the leaf microbiota with more than 50% of amplicon reads representing two  
30 bacterial species: WCS417 and *Flavobacterium* sp.. Co-inoculation experiments using  
31 WCS417 and At-LSPHERE *Flavobacterium* sp. Leaf82, suggest that the proliferation of these  
32 bacteria is influenced by both microbial and plant-derived factors. Together, our data connect  
33 systemic immunity with leaf microbiome dynamics and highlight the importance of plant-  
34 microbe-microbe interactions for plant health.

35  
36 **Keywords:** Plant immunity, phyllosphere microbiome, plant-microbe interactions, induced  
37 systemic resistance, plant growth-promoting bacteria, *Pseudomonas simiae*

38 **Introduction**

39 The functional traits introduced by the plant-associated microbiome are essential for plant  
40 growth and fitness and include nutrient acquisition as well as improved responses of the plant  
41 towards abiotic and biotic stressors (Berg, 2009; Schlaeppi & Bulgarelli, 2015). Some microbes  
42 are able to activate plant defence mechanisms, including systemic acquired resistance (SAR)  
43 and induced systemic resistance (ISR). While SAR is induced in systemic tissues of plants  
44 undergoing a local pathogen infection, ISR takes effect in aerial tissues of plants interacting  
45 with beneficial microbes in the rhizosphere (Vlot et al., 2020).

46 The molecular mechanisms of SAR are well-researched. SAR depends on two distinct but  
47 interwoven signalling pathways, one depending on salicylic acid (SA), the other on pipecolic  
48 acid (Pip) (Vlot et al., 2020). SA levels rise both locally and systemically after pathogen  
49 infection. This is driven by the enzymes ISOCHORISMATE SYNTHASE 1 (ICS1, also known  
50 as SID2) followed by the amidotransferase AvrPphB SUSCEPTIBLE3 (PBS3) (Rekhter et al.,  
51 2019; Vlot, Dempsey, & Klessig, 2009; Wildermuth, Dewdney, Wu, & Ausubel, 2001). Elevated  
52 SA levels lead to enhanced resistance through the action of downstream signalling  
53 intermediates, including the proposed SA receptors NON-EXPRESSOR OF  
54 PATHOGENESIS-RELATED PROTEINS1 (NPR1) and its paralogs NPR3 and 4 (Cao,  
55 Glazebrook, Clarke, Volko, & Dong, 1997; Y. Ding et al., 2018; Fu et al., 2012; Liu et al., 2020).  
56 In parallel, the non-proteinogenic amino acid Pip is synthesized in two steps by AGD2-like  
57 Defence Response Protein1 (ALD1) and SAR-DEFICIENT 4 (SARD4) and then converted to  
58 its presumed bioactive form *N*-hydroxy-pipecolic acid (NHP) (Chen et al., 2018; P. Ding et al.,  
59 2016; Hartmann et al., 2017; Hartmann et al., 2018; Navarova, Bernsdorff, Doring, & Zeier,  
60 2012). Notably, SA and Pip are believed to fortify each other's accumulation in a positive  
61 feedback loop, which depends on shared transcription (co-)factors, including NPR1 (Y. Kim,  
62 Gilmour, Chao, Park, & Thomashow, 2020; Sun et al., 2020).

63 The long-distance signal, which mediates the communication between local infected and  
64 systemic tissues and ultimately triggers the establishment of SAR, appears to be composed of  
65 multiple signalling intermediates, including SA, Pip, and/or NHP (reviewed in (Vlot et al., 2020)).  
66 Additionally, volatile signals such as the monoterpenes camphene and  $\alpha$ - and  $\beta$ -pinene are  
67 essential for SAR and propagate systemic immunity in SAR-induced as well as neighbouring  
68 plants (Riedlmeier et al., 2017; Wenig et al., 2019). GERANYL GERANYL DIPHOSPHATE  
69 SYNTHASE 12 (GGPPS12) is a key enzyme in the production of volatile monoterpenes in  
70 *Arabidopsis thaliana*. Mutations in this gene reduce monoterpene emissions and the capacity  
71 of the volatile emissions of these plants to support SAR (Riedlmeier et al., 2017). Perception  
72 of monoterpenes in SAR depends on the downstream SAR signalling intermediate LEGUME  
73 LECTIN-LIKE PROTEIN 1 (LLP1) (Breitenbach et al., 2014; Wenig et al., 2019).

74 ISR is elicited by plant growth-promoting bacteria or fungi in the rhizosphere (PGPR/PGPF),  
75 including, for example, several *Pseudomonas*, *Bacillus*, and *Trichoderma* strains (Pieterse et  
76 al., 2014; Vlot et al., 2020). In contrast to SAR, which provides protection against (hemi-)  
77 biotrophic pathogens, ISR protects above-ground tissues against both necrotrophic and (hemi-)  
78 biotrophic pathogens (Pieterse, van Wees, Hoffland, van Pelt, & van Loon, 1996; Ton, Van  
79 Pelt, Van Loon, & Pieterse, 2002; Van der Ent et al., 2008; Waller et al., 2005). The best-  
80 characterized ISR system to date is that induced in *Arabidopsis thaliana* upon interaction of  
81 the roots with *Pseudomonas simiae* WCS417r (Pieterse et al., 1996). The exact mechanism  
82 by which the presence of the microbes is perceived at the roots and relayed to the whole plant  
83 is not known at this point. The traditional idea is that ISR signals are propagated in the plant  
84 via jasmonic acid (JA)- and ethylene (ET)- dependent signalling (Pieterse et al., 1996; Pieterse  
85 et al., 1998; Pozo, Van Der Ent, Van Loon, & Pieterse, 2008). However, evidence is  
86 accumulating that there is no uniform ISR response to all PGPRs. Instead, there seem to be  
87 differing responses, depending on the eliciting microbial strains, involving JA/ET signalling as  
88 well as SA signalling pathways (Kojima, Hossain, Kubota, & Hyakumachi, 2013; Martínez-  
89 Medina et al., 2013; Nie et al., 2017; Niu et al., 2011; van de Mortel et al., 2012; Wu et al.,  
90 2018). These different responses are believed to enable the plant to react in a directed manner  
91 dependent on the lifestyle of the attacking pathogen (Nguyen et al., 2020). Signal propagation  
92 to the aerial tissues of the plant leads to so-called priming. During priming, full defence  
93 responses are not immediately activated. Rather, the plant raises a stronger and faster immune  
94 response after pathogenic challenge as compared to unprimed plants (U. Conrath, G. J. M.  
95 Beckers, C. J. G. Langenbach, & M. R. Jaskiewicz, 2015; Martinez-Medina et al., 2016; Mauch-  
96 Mani, Baccelli, Luna, & Flors, 2017).

97 The plant immune system influences the propagation of pathogens, but also that of non-  
98 pathogenic commensal or plant growth-promoting microbes, which are associated with the  
99 plant and together make up the plant microbiota (Teixeira, Colaianni, Fitzpatrick, & Dangl,  
100 2019). Local interactions of plant organs with pathogens can trigger long-distance signalling,  
101 for example from leaves to roots, and mediate changes in root exudates that influence the  
102 composition of the rhizosphere microbiota (Berendsen et al., 2018; Rudrappa, Czermek,  
103 Pare, & Bais, 2008; Yu, Pieterse, Bakker, & Berendsen, 2019). Similar changes in the plant  
104 immune status are associated with the dynamics of the phyllosphere microbiome (Chaudhry  
105 et al., 2020). Certain commensal bacteria from the phyllosphere, in turn, have been shown to  
106 enhance, for example, SA-associated immunity (Vogel, Bodenhausen, Gruissem, & Vorholt,  
107 2016). It thus seems conceivable that the plant immune system can modulate the phyllosphere  
108 microbiome, allowing the plant to 'exploit' beneficial properties of microbes to promote plant  
109 fitness.

110 In this study, we show that plant-microbe interactions in the rhizosphere influence the  
111 composition of the above-ground phyllosphere microbiome. We combine induced resistance  
112 assays in different *A. thaliana* genotypes with a molecular barcoding approach based on  
113 sequencing of amplified fragments of the 16S rRNA gene to assess the phyllosphere  
114 microbiome. The use of two different ISR inducers, *P. simiae* WCS417r and *Bacillus*  
115 *thuringiensis* var. *israelensis*, allows us to differentiate between local and systemic responses.  
116 Importantly, the data suggest that ISR-induced responses of the plant microbiome are  
117 influenced by interconnected microbe-microbe and microbe-plant interactions, which in  
118 response to *P. simiae* WCS417r reduce species diversity and thus presumably the stability of  
119 the leaf microbiome. Our results thus reveal a possible trade-off of ISR-based plant protection  
120 strategies and highlight the importance of tri-partite plant-microbe-microbe interactions for  
121 plant health.

122

## 123 **Methods**

124 Plant material and growth conditions.

125 In this study, *A. thaliana* ecotype Columbia-0 (Col-0) was used for all experiments. The mutants  
126 *lfp1-1*, *ggpps12*, *ald1*, *npr1-1*, *sid2*, and *jasmonate-insensitive 1 (jin1)* were previously  
127 described (Berger, Bell, & Mullet, 1996; Breitenbach et al., 2014; Cao et al., 1997; Riedlmeier  
128 et al., 2017; Song, Lu, McDowell, & Greenberg, 2004; Wenig et al., 2019; Wildermuth et al.,  
129 2001). All plants were grown from synchronised seeds. Plants were grown on normal potting  
130 soil (“Floradur® B Seed” (Floragard GmbH, Oldenburg, Germany) mixed with silica sand (grain  
131 size 0,6-1,2mm) at a ratio of 5:1. For ISR experiments seeds were surface-sterilized with 75%  
132 ethanol twice for 4 minutes and grown on ½ Murashige and Skoog medium for 10 days (d)  
133 prior to treatment and transfer to soil. Plants were grown in a 10 hour (h) day light regiment  
134 and a light intensity of 100 $\mu$ mol m<sup>-2</sup> s<sup>-1</sup> photosynthetically active photon flux density at 22°C  
135 during light periods and 18°C during dark periods. Relative humidity was kept at >70%.

136

## 137 ISR elicitors, Pathogens and Treatments

138 For elicitation of ISR, two different bacterial strains were used: *Pseudomonas simiae* WCS417r  
139 (Pieterse et al., 1996) and *Bacillus thuringiensis* var. *israelensis* (Goldberg, 1977). For ISR  
140 treatment, bacteria were grown on NB (Carl Roth, Karlsruhe, Germany) plates for 24 h and  
141 suspended in 10mM MgCl<sub>2</sub> to a final concentration of 10<sup>8</sup> colony forming units (cfu) mL<sup>-1</sup>,  
142 assuming that an OD<sub>600</sub> = 1 corresponds to 10<sup>8</sup> cfu mL<sup>-1</sup>. To induce ISR, the roots of 10-day-  
143 old seedlings were placed in wells of 96-well plates containing one of the bacterial suspensions  
144 or a sterile 10mM MgCl<sub>2</sub> control solution, each supplemented with 0.01% Tween-20 (v:v). After  
145 1 h of incubation, the seedlings were placed in pots with soil and grown to an age of 34 d. On  
146 the 34<sup>th</sup> day after sowing, the leaves of the plants were either harvested for further analysis or

147 inoculated with  $10^5$  cfu mL $^{-1}$  of *Pseudomonas syringae* pathovar *tomato* (*Pst*), which was  
148 maintained and used for infections as previously described (Wenig et al., 2019). To determine  
149 bacterial growth in the plants, *Pst* titers were determined 4 days post-inoculation (dpi). To this  
150 end, leaf discs punched out of the infected leaves were incubated in 10mM MgCl<sub>2</sub> + 0,01%  
151 Silwet (v:v) for 1 h at 600 rpm. The resulting bacterial suspensions were serially diluted in steps  
152 of 10x. 20 $\mu$ l per dilution were plated on NYGA agar plates (Wenig et al., 2019) and incubated  
153 for 2 d at room temperature. Bacterial titers were calculated based on the number of bacterial  
154 colonies.

155 Leaf inoculations were performed using 4-5-week-old plants. *Flavobacterium* sp. was obtained  
156 as strain Leaf82 from the At-LSPHERE synthetic community (Bai et al., 2015) and maintained  
157 on NB medium. Syringe infiltration was performed using  $10^5$  cfu mL $^{-1}$  of bacteria in 10 mM  
158 MgCl<sub>2</sub>. Spray inoculation was performed using  $10^8$  cfu mL $^{-1}$  of bacteria in 10 mM MgCl<sub>2</sub>  
159 supplemented with 0.01% Tween-20 (v:v). *In planta* bacterial titers were determined as  
160 described above by counting plate-grown bacterial colonies derived from inoculated leaves.  
161 The colonies of WCS417 and Leaf82 were distinguished based on colour differences.

162 SAR was induced in 4-5-week-old plants as previously described (Wenig et al., 2019) except  
163 that WCS417 or Bti were used for the primary inoculation of the first two true leaves of the  
164 plants by syringe infiltration of  $10^6$  cfu mL $^{-1}$  of bacteria in sterile 10 mM MgCl<sub>2</sub>.  $10^6$  cfu mL $^{-1}$  of  
165 *Pst* carrying the effector *AvrRpm1* was used as the positive control and 10 mM MgCl<sub>2</sub> as the  
166 negative control treatment (Wenig et al., 2019). Three d later, the establishment of SAR was  
167 tested by a secondary infection of the third and fourth true leaf of the plants with  $10^5$  cfu mL $^{-1}$   
168 of *Pst*. *Pst* titers were determined at 4 dpi as described above.

169

#### 170 RNA extraction and RT-qPCR analysis

171 RNA was isolated with Tri-Reagent (Sigma-Aldrich, St. Louis, USA) according to the  
172 manufacturer's instructions. cDNA was generated with SuperscriptII reverse transcriptase  
173 (Invitrogen, Carlsbad, USA). Quantitative PCR (qPCR) was performed using the Sensimix  
174 SYBR low-rox kit (Bioline, Memphis, USA) on a 7500 real-time PCR system (Applied  
175 Biosystems, Foster City, USA). Primers that were used for qPCR are listed in Supplementary  
176 Table S1. Transcript accumulation of target genes was analyzed using Relative Quantification  
177 with the 7500 Fast System Software 1.3.1.

178

#### 179 DNA-Isolation, PCR and Amplicon Sequencing

180 100-200ng of leaf material was freeze-dried for 24 h at -40°C and 0.12mbar (Alpha 2-4 LD  
181 Plus, Martin Christ Gefriertrocknungsanlagen, Osterode, Germany). DNA isolation was  
182 performed utilizing the FastPrep Soil Kit (MPbio) according to manufacturer's instructions after  
183 an additional step of leaf grinding using a tissue lyser (Retsch, Haan, Germany) and glass

184 beads (1mm diameter) at 25Hz for two minutes. Following DNA extraction, the variable regions  
185 V5-V7 of the bacterial 16S rRNA gene were amplified by PCR (NEBnext High Fidelity 2x  
186 Master Mix, New England Biolabs, Ipswich, MA, USA) using 10 ng of DNA per reaction and  
187 the primers 799F and 1193R from (Bulgarelli et al., 2012; Chelius & Triplett, 2001).  
188 Three independent PCR reactions were performed per DNA sample using the following  
189 conditions: 98°C for 30 s, 98°C for 10 s, 58°C for 20 s, 72°C for 20 s, 72°C for 2 m. Steps 2-4  
190 were repeated 25 times. The resulting PCR amplicons were subjected to gel electrophoresis  
191 to separate amplicons derived from bacteria and chloroplasts, since chloroplast yield longer  
192 amplicons than bacterial DNA. The DNA amplicons derived from the bacterial 16S rRNA gene  
193 were extracted from the gels using the QIAquick Gel Extraction Kit (Qiagen, Hilden, Germany).  
194 After determination of the DNA concentration of each amplicon (nanodrop, Implen, Munich,  
195 Germany), the 16S rRNA gene amplicons from 3 replicates per sample were pooled at  
196 equimolar amounts. The fragment sizes and concentrations of the pooled samples were  
197 determined on a Fragment analyzer 5200 using the DNF-473-Standard Sensitivity NGS  
198 Fragment Analysis Kit (Agilent, Santa Clara, CA, USA). The indexing PCR was performed  
199 under the following conditions: 98°C for 10 s, 55°C for 30 s and 72°C for 30 s and final  
200 extension at 72°C for 5 min. Each PCR reaction contained 1x NEBNext High Fidelity  
201 Mastermix, 10 ng of template DNA and index primer 1 (N7xx) and index primer 2 (N5xx) of  
202 Nextera XT Index Kit v2 Set A (Illumina, San Diego, CA, USA) according to the manufacturer's  
203 instruction. All samples were purified using MagSi NGSprep Plus Beads (Steinbrenner,  
204 Wiesenbach, Germany). Samples were validated and quantified on a Fragment analyzer 5200  
205 using the DNF-473-Standard Sensitivity NGS Fragment Analysis Kit, diluted and pooled to a  
206 final concentration of 4 nM for the sequencing run on Illumina MiSeq using the MiSeq Reagent  
207 Kit v3 (600-cycle). Demultiplexing was done using the MiSeq Reporter Software v 2.6.  
208 (Illumina).

209

## 210 Statistical analysis

211 All statistical analyses were done using R version 3.6.3.(R Development Core Team, 2020).  
212 For the analysis of bacterial titers, a Shapiro wilk test for normal distribution showed, that the  
213 cfu counts resulting from the infection assays did not follow normal distribution ( $\alpha=0.05$ ).  
214 Therefore, a Kruskal-Wallis test was used to test for significance at  $\alpha=0.05$ , followed by a post  
215 hoc pairwise Wilcox test with correction for multiple testing using the Benjamini&Hochberg  
216 method.

217

## 218 Amplicon data analysis

219 Pre-processing of the amplicon data was performed using the package "dada2", including  
220 removal of low-quality reads, merging of reads, chimera removal and taxonomic assignment

221 based on the Silva Seeds v138 database (Callahan BJ, 2016; Yilmaz et al., 2013). Taxonomy  
222 assignments were performed based on Amplicon Sequence Variants (ASVs). Phylogenetic  
223 trees were fitted based on DECIPHER (Wright, 2016). To control for uniformity of DNA isolation  
224 and PCR bias as well as contamination, a commercially available Microbial Community  
225 Standard by ZymoBIOMICS was prepared as an additional sample and handled in the same  
226 fashion as the other samples after the freeze-drying step.

227 Prior to analysis of the data, we mined the *Pst* titer reductions triggered by each treatment as  
228 compared to the appropriate controls, and excluded data from samples derived from  
229 experiments, in which ISR was not significant. Data from the remaining 6-7 replicates per  
230 treatment were analysed using the R packages Vegan, Phyloseq, DESeq2, and Phangorn  
231 were used (Holmes, 2013; Jari Oksanen, 2019; Love, 2014; Schliep, Potts, Morrison, & Grimm,  
232 2017). Read counts were normalized to the read count per sample. Alpha diversity was  
233 calculated using the Shannon's- as well the Simpson's index (Phyloseq). Nonmetric  
234 Multidimensional Scaling (NMDS) was plotted after calculation of Unifrac-distances  
235 (Phyloseq). Based on these analyses and Grubbs outlier tests ( $p < 0.05$ ), we excluded the data  
236 from one sample per treatment, which were outliers in terms of species-richness in comparison  
237 to the other samples of the respective treatments. Differentially abundant ASVs were  
238 determined using DESeq2, limiting the analysis to ASVs present in at least three samples.

239

## 240 **Results**

241 *Bacillus thuringiensis* var *israelensis* (*Bti*) elicits ISR in *A. thaliana*

242 *P. simiae* WCS417r, referred to below as WCS417, triggers ISR in *A. thaliana*, reducing the  
243 propagation of pathogenic *P. syringae* pathovar *tomato* (*Pst*) in the leaves of the treated plants  
244 (Pieterse et al., 1996). Here, we tested if treatment of *A. thaliana* roots with *Bti* has a similar  
245 effect. To this end, 10-day-old, sterile-grown seedlings were treated with *Bti* or with WCS417  
246 as a positive control or with sterile 10mM MgCl<sub>2</sub> as a negative control. The treated seedlings  
247 were transferred to soil, and leaves of the resulting plants were inoculated with *Pst*. As  
248 expected, treatment of *A. thaliana* roots with WCS417 reduced the growth of the *Pst* inoculum  
249 in the leaves as compared to that in control plants, indicating the induction of ISR in response  
250 to WCS417 (Fig. 1A). Treatment of seedling roots with *Bti* caused a comparable reduction of  
251 *Pst* growth in the leaves (Fig. 1A), indicating that *Bti* induced ISR in *A. thaliana*.

252 In contrast to SAR, which is classically associated with SA signalling, WCS417-induced ISR  
253 has previously been associated with JA signalling (Pieterse et al., 1996; Pieterse et al., 1998;  
254 Pozo et al., 2008). *PLANT DEFENSIN 1.2* (*PDF1.2*) and *VEGETATIVE STORAGE PROTEIN*  
255 *2* (*VSP2*) are marker genes of the MYC2-independent and MYC2-dependent JA signalling  
256 pathways, respectively (Pieterse, Van der Does, Zamioudis, Leon-Reyes, & Van Wees, 2012).  
257 Here, we tested whether ISR induction leads to changes in JA signalling by conducting RT-

258 qPCR analysis of *PDF1.2* and *VSP2* transcript accumulation. Additionally, we tested a possible  
259 influence of ISR on SA signalling targeting the SA marker gene *PATHOGENESIS RELATED*  
260 *1 (PR1)* (van Loon, Rep, & Pieterse, 2006). We sampled leaves of *Bti*-, WCS417-, and control-  
261 treated plants prior to a pathogenic challenge with *Pst* and 6 h post infection. *PDF1.2*, *VSP2*,  
262 and *PR1* transcript accumulation in *Bti*- as well as WCS417-treated plants was not significantly  
263 different in comparison to that in control-treated plants (Fig. 1B, upper panel). Thus, the  
264 induction of ISR did not induce transcript accumulation of these genes. Similarly, *PDF1.2*,  
265 *VSP2*, and *PR1* transcript accumulation was not different in ISR-induced as compared to  
266 control-treated plants sampled 6 h after challenge inoculation of the leaves with *Pst* (Fig. 1B,  
267 lower panel), indicating that transcript accumulation was not primed by either of the ISR  
268 treatments. Thus, under the experimental conditions used here, both *Bti* and WCS417  
269 triggered ISR against *Pst* in *A. thaliana* in the absence of detectable induction or priming of JA  
270 and SA marker genes.

271

#### 272 Varying molecular requirements for WCS417- and *Bti*-induced ISR

273 WCS417-induced ISR has been shown to depend on functional MYC2-associated JA  
274 defences, but not on the accumulation of SA (Pieterse et al., 1996; Pieterse et al., 1998; Pozo  
275 et al., 2008). Here, we compared the functionality of ISR induced by *Bti* as compared to  
276 WCS417 in *A. thaliana* mutants with compromised JA defences (*jin1/myc2*) and also in mutants  
277 with compromised SA accumulation (*sid2*) and signalling (*npr1*). ISR was induced as described  
278 above, and the leaves of the plants were inoculated with *Pst*. Col-0 wild type supported less  
279 *Pst* growth in the leaves of plants pre-treated with either WCS417 or *Bti* as compared to the  
280 controls, confirming that ISR was induced in response to both bacterial strains (Fig. 2A). As  
281 reported before (Nickstadt, 2004), the *jin1 (myc2)* mutant supported less *Pst* growth than Col-  
282 0 wild type plants (Fig. 2A). In accordance with previous findings (Pozo et al., 2008), WCS417-  
283 induced ISR was compromised in *jin1* mutant plants (Fig. 2A). Similarly, *Bti*-induced ISR was  
284 abolished in *jin1* plants resulting in similar or slightly elevated growth of the *Pst* challenge  
285 inoculum as compared to that observed in control-treated plants. Thus, the *JIN1*-encoded, JA-  
286 associated transcription factor MYC2 is essential for ISR triggered by both WCS417 and *Bti*.  
287 Similarly, neither WCS417 nor *Bti* treatments reduced the *Pst* titers in the leaves of *sid2* or  
288 *npr1* mutant plants (Fig. 2A). This suggests that ISR induced by both WCS417 and *Bti* under  
289 the experimental conditions used here, depends on functional pathogen-induced SA  
290 accumulation and signalling.

291 Recent evidence suggests roles of SAR-associated signalling intermediates in ISR (Cecchini,  
292 Steffes, Schlappi, Gifford, & Greenberg, 2015; Shine et al., 2019). Here, we assessed the  
293 involvement of Pip-dependent pathways in ISR by using *ald1* mutant plants with defects in Pip  
294 biosynthesis (Navarova et al., 2012). We also tested the involvement of SAR-associated

295 volatile monoterpenes as well as their perception by monitoring ISR in the respective loss-of-  
296 function mutants *ggpps12* and *lfp1* (Wenig et al., 2019). In comparison to the respective control  
297 treatments, treatment of *ald1* and *ggpps12* plants with *Bti* resulted in decreased *Pst* titers,  
298 suggesting that ISR had been induced in these plants (Fig. 2B). In contrast, treatment of the  
299 same mutants with WCS417 did not reduce growth of the *Pst* challenge inoculum, indicating  
300 that WCS417-triggered ISR was compromised in *ald1* and *ggpps12* mutant plants. This implies  
301 the involvement of Pip as well as monoterpenes in the realisation of immunity in WCS417-  
302 dependent ISR. In contrast to WCS417, *Bti* triggered ISR by a mechanism relying on the SAR-  
303 associated signalling factor LLP1: the *Pst* challenge inoculum grew to similar titers in the leaves  
304 of *Bti*-treated compared to control-treated *lfp1* mutant plants (Fig. 2B). Taken together, the data  
305 suggest that WCS417 and *Bti* trigger ISR via two at least partially distinct mechanisms.  
306

307 Microbial composition of the phyllosphere differs in dependency of the ISR-eliciting bacterial  
308 strain

309 To address the question, whether the composition of the microbiome changes in leaves of  
310 plants undergoing ISR, we performed amplicon sequencing of the bacterial 16S rRNA gene.  
311 To this end, we treated plants at the age of 10 days with either *Bti*, WCS417, or MgCl<sub>2</sub> as the  
312 control. 3½ weeks later, we harvested the leaves, isolated the DNA, and amplified and  
313 sequenced the regions V5-V7 of the 16S rRNA gene. In total 830.276 reads were sequenced.  
314 After data pre-processing (see Methods), the remaining 622.234 reads, averaging 36.602  
315 reads per sample, were assigned to 1844 amplicon sequence variants (ASVs) acting as a  
316 proxy for bacterial species. Per sample 110 to 432 ASVs were identified. To assess the bias  
317 introduced by DNA isolation and PCR as well as to detect contaminations, we additionally  
318 processed a commercially available bacterial standard (ZYMO, see Methods). The microbial  
319 standard revealed no gross bias with respect to sequencing reads per bacterial group and only  
320 a slight contamination by a *Ralstonia* sp. (Supplementary Fig. S1). This data suggests that our  
321 samples were not subject to significant bias or contamination during DNA isolation as well as  
322 replication.

323 To obtain a general overview of the microbial composition of our samples, we first examined  
324 the sequencing data on the phylum level. Among the ten most abundant phyla were  
325 Proteobacteria, Firmicutes, Bacteroidetes and Actinobacteria (Fig. 3), which correspond to the  
326 phyla which were previously described as “core-phyla” for the microbiome of plants’  
327 phyllosphere (Lundberg et al., 2012; Vorholt, 2012). Additionally, high counts of Cyanobacteria  
328 were detected, mainly caused by one ASV. This is rather unusual and presumably due to high  
329 air humidity during plant growth. The remaining phyla of high abundance were Myxococcota,  
330 Gemmatimonadota, Bdellovibrionota, Acidobacteria and Abditibacteriota. We detected  
331 differences in the phylum composition between the treatments. WCS417-treated plants

332 contained more Bacteroidota and less Actinobacteria than control- and *Bti*-treated plants (Fig.  
333 3).

334

335 The microbiome of WCS417-treated plants displays reduced species diversity

336 In the next step, we examined the ASVs by plotting a rarefaction curve of the amplicon data.  
337 The rarefaction curve confirmed a sufficient sequencing depth by showing a clear saturation  
338 of the curves (Fig. 4A). Additionally, the rarefaction curves revealed a significantly lower  
339 number of ASVs in WCS417-treated plants in comparison to *Bti*- or control-treated plants. The  
340 microbiomes of WCS417-treated plants on average contained 165 ASVs per sample in  
341 comparison to 331 or 361 ASV per sample in *Bti*- and control-treated plants, respectively (Fig.  
342 4A). Therefore, we analysed ASV richness and evenness utilizing the Shannon's Index  
343 (Spellerberg & Fedor, 2003) and dominance of single ASVs using the Simpson's Index  
344 (Simpson, 1949). The apparent lower species richness in WCS417-treated plants was  
345 confirmed by the Shannon's Index, which was significantly lower ( $p<0.05$ ) in WCS417-treated  
346 plants than in *Bti*- or control-treated plants (Fig. 4B). The Simpson's Index, which does not  
347 account for species richness but rather for dominance of single species, did not reveal  
348 significant differences between the treatments (Fig. 4B). Thus, species diversity was reduced  
349 in the leaf microbiome of WCS417-treated plants, while dominance by species was not  
350 different from that in *Bti*- and control-treated plants.

351

352 Nonmetric multidimensional scaling reveals differences and similarities of bacterial  
353 composition between the different treatments

354 In the next step, we addressed the question, how similar or distinct the different samples are  
355 with regards to their composition under consideration of the relative relatedness of the different  
356 ASVs. To this end, we calculated weighted Unifrac-distances (Lozupone & Knight, 2005) and  
357 performed a nonmetric multidimensional scaling to see whether the samples cluster for  
358 example by treatment or replicate number. The non-metric multidimensional scaling shows  
359 that the microbiome of plants treated with WCS417 clustered distinctly from that of *Bti*- and  
360 control-treated plants (Supplementary Fig. S2). Despite the similar clustering between the *Bti*  
361 and control treatments, both groups of samples clustered in a significantly different manner. In  
362 some samples we observed a slight clustering according to the experimental replicate (e.g.,  
363 number 6 and number 7). This hints at possible batch effects due to treatment, growth, or  
364 sampling of the plants.

365

366 Occurrence of ISR-eliciting bacterial strains on the ISR-treated plants

367 We wanted to analyze if the bacterial strains we used to elicit ISR also occurred on the leaves  
368 of the plants. Therefore, we examined the absolute numbers of ASV3 and ASV953, whose

369 16S rRNA gene sequences correspond to that of WCS417 and *Bti*, respectively. In WCS417-  
370 treated plants, the reads of WCS417 on the leaves make up ~25% of the reads per sample,  
371 averaging nearly 10.000 reads per sample (Fig. 5A). This suggests a possible contamination  
372 of the phyllosphere with WCS417. Alternatively, it is possible that WCS417 actively proliferates  
373 on *A. thaliana* leaves. In support of the latter hypothesis, we detected moderate growth of a  
374 WCS417 inoculum in *A. thaliana* leaves (Supplementary Fig. S3). While absent from control-  
375 treated plants, WCS417 was found with up to 100-1000 reads per sample in leaves of *Bti*-  
376 treated plants (Figure 5A), suggesting a possible recruitment of WCS417 to the phyllosphere  
377 of *Bti*-treated plants. In *Bti*-treated plants, *Bti* was detected with 7 reads in a single sample (Fig.  
378 5A). Also, 14 reads corresponding to *Bti* were detected in one sample from control-treated  
379 plants. This finding suggests that contamination of the phyllosphere during the ISR-inducing  
380 treatment had been negligible. Upon inoculation of *A. thaliana* leaves with *Bti*, we observed  
381 that the titers stagnated over time (Supplementary Fig. S3), suggesting that *Bti* does not  
382 proliferate in *A. thaliana* leaves. Taken together, inoculation of *A. thaliana* roots with ISR-  
383 inducing bacteria resulted in proliferation of WCS417, but not *Bti*, on the leaves of the treated  
384 plants. Strikingly, the data suggest that *Bti*-triggered ISR was accompanied by the recruitment  
385 of WCS417 to the phyllosphere.

386

387 Different bacterial groups are enriched in the phyllosphere depending on the treatment

388 For the analysis of ASVs that appeared in significantly different abundance between  
389 treatments, only ASVs that were detected in at least three samples per treatment were taken  
390 into account. We utilized the R package “dada2” which was originally created for the analysis  
391 of RNAseq-data. This library has the advantage of utilizing more suitable methods for data  
392 normalization than the package “Phyloseq”, which we used for most of the remaining data  
393 analysis. In this manner, data normalization was independent of subsampling and the  
394 associated loss of data (McMurdie & Holmes, 2014).

395 In comparison to control-treated plants, *Bti*-treated plants displayed differential abundance of  
396 14 ASVs and WCS417-treated plants of 42 ASVs (Supplementary Table S2). Most of the  
397 differentially accumulating ASVs were less abundant in ISR-treated compared to control-  
398 treated plants. Also, most of the significantly different ASVs were detected at relatively low  
399 read count numbers of 1000 reads in total or less. In contrast, two bacterial species were  
400 considerably enriched in the ISR-treated plants. In samples from WCS417-treated plants, a  
401 *Flavobacterium* sp. was detected at an average of 6000 reads per sample, while the same  
402 strain was detected with an average of 110 reads per sample in *Bti*-treated plants (Fig. 5B).  
403 By comparison, the same ASV was detected with 1 read in 1 control sample, and thus  
404 remained negligible on control-treated plants (Fig. 5B). Similarly, *Bti*-treated plants displayed  
405 a significant accumulation of a *Solimonas terraee* strain, which was detected in 4 out of 5

406 samples with an average of 231 reads per sample (Fig. 5B). The same ASV occurred in 1  
407 sample each from control- and WCS417-treated plants. Taken together, ISR triggered by  
408 WCS417 and *Bti* was associated with enrichment of the phyllosphere microbiome with  
409 WCS417 and *Flavobacterium sp.*, while *Bti* treatment additionally resulted in the enhanced  
410 recruitment of *S. terra*e to the *A. thaliana* phyllosphere.

411

#### 412 Microbe-microbe-host interactions in the *A. thaliana* phyllosphere

413 Because WCS417 proliferated in *A. thaliana* leaves, we tested if this proliferation triggered  
414 systemic immunity against *Pst*. To this end, we infiltrated the first true leaves of 4-5-week-old  
415 *A. thaliana* plants with WCS417 or with MgCl<sub>2</sub> as the negative control. As a positive control,  
416 we used the bacterial strain *Pst/AvrRpm1* which is known to cause SAR (Breitenbach et al.,  
417 2014). Three days later, we performed a challenge infection of the systemic leaves with *Pst*.  
418 In comparison to the negative control treatment, *Pst/AvrRpm1* pre-treatment significantly  
419 decreased *Pst* propagation, indicating that SAR had been induced (Supplementary Fig. S4).  
420 In contrast, a local WCS417 leaf inoculation did not decrease *Pst* titers in the systemic tissue  
421 of the treated plants. Similar experiments using *Bti* as the primary, SAR-inducing treatment  
422 showed that a local leaf inoculation with *Bti* triggered SAR in systemic leaves (Supplementary  
423 Fig. S4). Thus, when inoculated onto *A. thaliana* leaves, *Bti*, but not WCS417, induced  
424 systemic immunity.

425 We next investigated if WCS417 locally enhances the immunity of *A. thaliana* leaves against  
426 *Pst*. Because the relative abundance of *Flavobacterium sp.* was significantly enhanced on the  
427 leaves of ISR-induced plants, we also tested if this bacterium affects defence. To this end, we  
428 used bacterial strain Leaf82 from the *At-LSPHERE* collection (Bai et al., 2015), which displays  
429 100% sequence identity of its V5-V7 16S rRNA gene region with that of *Flavobacterium sp.* To  
430 study induced resistance, WCS417 and Leaf82 were syringe-infiltrated into leaves of 4-5-  
431 week-old *A. thaliana* plants. Two days later, the same leaves were infiltrated with *Pst*. In  
432 comparison to the control treatment, WCS417 treatment of the leaves caused a reduction of  
433 *Pst* proliferation (Fig. 6A), suggesting that WCS417 locally induced resistance on *A. thaliana*  
434 leaves. Because WCS417-induced resistance was not observed in *npr1* mutant plants (Fig.  
435 6A), the observed reduction of *Pst* growth was likely associated with plant immunity. In  
436 contrast, Leaf82 treatment did not reduce *Pst* proliferation on the leaves and thus did not  
437 enhance plant defences against this pathogen (Fig. 6B).

438 Finally, we studied if the local WCS417-induced defence response of *A. thaliana* influenced  
439 the proliferation of Leaf82. To this end, we performed the same induced resistance experiment  
440 as above. Two days after treating leaves with WCS417 or a control solution, we infiltrated the  
441 same leaves with Leaf82. Although WCS417-induced ISR was associated with enhanced  
442 proliferation of *Flavobacterium sp.* on the leaves, leaf inoculation of WCS417 did not cause

443 enhanced growth of a subsequent Leaf82 inoculum (Fig. 6C). Although it thus seems as though  
444 WCS417 does not affect Leaf82 through plant responses, the proliferation of Leaf82 was  
445 reduced on *npr1* mutant as compared to wild type plants (Fig. 6C). Similarly, WCS417  
446 proliferated less on *npr1* mutant than on wild type plants (Supplementary Fig. S5). Taken  
447 together, the data suggest that WCS417 activates *NPR1*-dependent responses in plants that  
448 reduce growth of pathogenic *Pst* and at the same time enhance WCS417 proliferation.  
449 Because *Flavobacterium* sp. or Leaf82 titers on leaves appear to correlate with those of  
450 WCS417 in various treatments (Figs. 5, 6C, and S5), the data suggest that this bacterium is  
451 under direct influence of WCS417 and thus, during ISR, subject to plant-microbe-microbe  
452 interactions.

453

#### 454 **Discussion**

455 We showed here that *Bacillus thuringiensis israelensis* (*Bti*) triggers ISR in *A. thaliana*.  
456 Additionally, local leaf application of *Bti* enhanced immunity in systemic leaves of the treated  
457 plants. Until now, *Bti* has been known mainly for its CRY-proteins, which are toxic specifically  
458 for insects and are widely used as crop protection agents in agriculture (Bravo, Gill, & Soberón,  
459 2007). ISR-eliciting properties of *Bacillus thuringiensis* subspecies have so far been observed  
460 in tomato (Hyakumachi et al., 2013; Raddadi et al., 2007; Takahashi et al., 2014). Our data  
461 suggest that *Bti* enhances systemic immunity in *A. thaliana* by inducing both root-to-leaf and  
462 leaf-to-leaf systemic immune signalling.

463 *Bti*-triggered ISR depends on functional JA and SA signalling and on LLP1, which is also  
464 essential for SAR (Breitenbach et al., 2014). ISR triggered by the model strain WCS417  
465 depended on SA and JA signalling and further on Pip and monoterpene biosynthesis (Figure  
466 2). Until recently, SAR and ISR were believed to depend on different molecular mechanisms.  
467 Recent evidence, however, suggests that a number of SAR-associated defence cues also  
468 promotes ISR (Vlot et al., 2020). These cues include azelaic acid, AZELAIC ACID INDUCED1,  
469 and glycerol-3-phosphate (Cecchini et al., 2019; Cecchini et al., 2015; Shine et al., 2019),  
470 which act downstream of Pip in SAR (Wang et al., 2018). Here, Pip promoted ISR triggered by  
471 WCS417, but not *Bti*. Pip and glycerol-3-phosphate further cooperate to drive monoterpene  
472 emissions during SAR (Wenig et al., 2019). Consequently, monoterpene emissions promoted  
473 the same WCS417-triggered ISR mechanism as Pip. Although LLP1 promotes SAR in a  
474 positive feedback loop with Pip (Wenig et al., 2019), this function of LLP1 does not appear  
475 involved in WCS417-triggered ISR. It is possible that another function of LLP1, which we  
476 previously connected with local release of SAR-associated long-distance signals (Wenig et al.,  
477 2019), is important for ISR triggered by *Bti*. Together, this work suggests functions of three  
478 SAR-associated signalling intermediates in ISR, supporting the hypothesis that the  
479 mechanisms of SAR and ISR are not as different as traditionally believed.

480 Under our experimental conditions, WCS417 appears to be recruited to the phyllosphere, when  
481 applied to roots (Figure 5). There, the bacteria proliferate (Supplementary Fig. S3), and  
482 potentially enhance the immunity of the leaves against *Pst* via a local induced resistance  
483 response (Figure 6). This contrasts with findings of Pieterse et al. (1996, 1998) who showed  
484 that WCS417 remains confined to the rhizosphere during the elicitation of ISR. WCS417-  
485 triggered ISR further was functional in SA-deficient *NahG* plants (Pieterse et al., 1996),  
486 whereas the same response was compromised in *sid2* plants with reduced pathogen-induced  
487 SA biosynthesis (Figure 2)(Wildermuth et al., 2001). These contrasting results could be a  
488 consequence of the differential WCS417 proliferation on leaves in our studies. Alternatively,  
489 the combined data suggest a possible role of low remaining SA levels or SA-derivatives such  
490 as MeSA, which accumulate in *NahG* plants, in WCS417-triggered ISR (Lim et al., 2020; Park,  
491 Kaimoyo, Kumar, Mosher, & Klessig, 2007). In accordance with previous findings (Pozo et al.,  
492 2008), the WCS417-triggered ISR response further relied on functional MYC2-dependent JA  
493 signalling (Figure 2), suggesting synergism between SA and JA in ISR-activated leaves.  
494 ISR not only affects the plant itself, but also seems to change the habitat it provides in its  
495 phyllosphere, leading to changes in the microbial composition of the leaf. Here, ISR was  
496 associated with a higher relative abundance of WCS417 and *Flavobacterium* sp. in the *A.*  
497 *thaliana* phyllosphere. *Bti* additionally triggered a distinct enrichment of a *Solimonas terrae*  
498 strain first isolated in soil from Korea (S.-J. Kim et al., 2014). Until now, not much is known  
499 about this and the other five known species of the genus *Solimonas*. Recently, *Solimonas*  
500 *terrae* was associated with changes in the microbiome of plants after a growth-stimulating cold  
501 plasma treatment in *A. thaliana* (Tamošiūnė et al., 2020). Here, proliferation of *S. terrae*  
502 appeared uniquely related to the ISR trigger *Bti*, and thus might be responsive to true systemic  
503 signalling. In future, it will be of interest to investigate possible beneficial properties of this  
504 bacterial strain for plant health.  
505 In the phyllosphere of WCS417-treated plants, WCS417 and *Flavobacterium* sp. together  
506 accounted for more than 50% of the sequenced reads. Consequently, the relative abundance  
507 of other bacterial strains was reduced, possibly because they were supplanted by WCS417  
508 and *Flavobacterium* sp. Species belonging to the phylum Proteobacteria have been proposed  
509 to act as 'key-stone' bacterial species in phyllosphere microbiomes (Carlstrom et al., 2019).  
510 Single 'key-stone' strains can have significant effects on the overall microbial composition.  
511 However, Leaf82, the strain highly similar to the *Flavobacterium* sp. we found enriched in  
512 association with WCS417, does not appear to be significantly influenced by  
513 Gammaproteobacteria related to WCS417 (Carlstrom et al., 2019). Here, consecutive leaf  
514 inoculations of WCS417 and Leaf82 suggest that Leaf82 proliferation is influenced by  
515 WCS417, suggesting direct microbe-microbe interactions between these strains in the *A.*  
516 *thaliana* phyllosphere.

517 Notably, the phyllosphere microbiome of WCS417-treated plants displayed a significantly  
518 reduced species richness. Because lower richness in microbiota has been associated with a  
519 lower stability of the microbiome and a higher risk of dominance by pathogens (Chaudhry et  
520 al., 2020; Tao Chen et al., 2020; Ives & Hughes, 2002), this suggests a possible trade-off of  
521 ISR in plants. In this respect, it seems of interest that we detected considerably less significant  
522 shifts in the phyllosphere microbiome composition than Chen et al. (2020), who studied the  
523 influence of local immune response driven by pathogen-associated molecular patterns  
524 (PAMPs). The comparatively moderate phyllosphere microbiome changes in response to ISR  
525 likely reflect the fact that ISR is established as a form of priming (U. Conrath, G. J. Beckers,  
526 C. J. Langenbach, & M. R. Jaskiewicz, 2015; Mauch-Mani et al., 2017). During priming, the  
527 bulk of defence-associated molecular responses do not become evident before a pathogen  
528 challenge (Martinez-Medina et al., 2016). Therefore, it is not unexpected that the microbiome  
529 also displays only a moderate response to the induction of ISR. By comparison, *A. thaliana*  
530 mutants, which were defective in the MIN7-vesicle-trafficking pathway and incapable of  
531 mounting PAMP-triggered immunity (PTI), displayed more significant shifts in the relative  
532 abundance of Proteobacteria (up) and Actinobacteria (down). Deployment of this “incorrectly”  
533 assembled microbiome onto gnotobiotic plants led to necrosis and stunted plant growth (T.  
534 Chen et al., 2020). These findings associate compromised PTI responses with reduced plant  
535 fitness, caused by changes in the phyllosphere microbiome. In our experiments, although  
536 WCS417 reduced the species richness of the phyllosphere microbiome, defence against *Pst*  
537 was enhanced. Notably, we focused on the bacterial part of the microbiome, and cannot  
538 exclude possible additional effects of e.g. fungi and other eukaryotic microbes (Chaudhry et  
539 al., 2020).

540 Recruitment of WCS417 to the phyllosphere appears to be an active process driven by NPR1-  
541 mediated plant immunity. Data shown in Figure 6 suggest that enhanced proliferation of  
542 WCS417, in turn, drives proliferation of *At-LSPHERE Flavobacterium sp.* Leaf82. Species  
543 belonging to the genus *Flavobacterium* are known to be well-adapted to the phyllosphere,  
544 living epi- as well as endophytically on *A. thaliana* plants (Bodenhausen, Horton, & Bergelson,  
545 2013). They are capable of metabolizing complex carbon-sources such as pectin,  
546 hemicellulose, and peptidoglycan components of gram-positive cell-walls of bacteria (Kolton,  
547 Sela, Elad, & Cytryn, 2013; Peterson, Dunn, Klimowicz, & Handelsman, 2006). By those  
548 attributes, *Flavobacterium* spp. can outcompete other bacterial groups. Additionally, they have  
549 been assigned enhanced biocontrol as well as plant growth-promoting properties.  
550 *Flavobacterium* spp., for example, produce cyanide acting as an antimicrobial agent as well as  
551 compounds that act as plant growth-promoting hormones, including auxins, gibberellins and  
552 cytokinins (Gunasinghe, Ikiriwatte, & Karunaratne, 2004; Hebbar, Berge, Heulin, & Singh,

553 1991; Maimaiti et al., 2007; Sang & Kim, 2012). It is thus conceivable that ISR triggers the  
554 recruitment of plant growth-promoting microbiota to the phyllosphere.

555

## 556 Conclusions

557 ISR triggered in *A. thaliana* by *Bti* or WCS417 leads to the recruitment of microbiota with plant  
558 growth-promoting properties to the phyllosphere. This recruitment depends on interconnected  
559 plant-microbe and microbe-microbe interactions. WCS417-triggered ISR reduces the species  
560 richness of the phyllosphere microbiome, which hints at a possible trade-off of ISR in plants.  
561 Whereas short term effects did not appear to enhance plant disease susceptibility, further  
562 investigations are necessary to gain insights into the long-term effects of these plant-microbe-  
563 microbe interactions on plant health.

564

## 565 Acknowledgements

566 The authors thank Dr. Michael Rothbauer (Institute of Network Biology, Helmholtz Zentrum  
567 Muenchen, Germany) for providing *Bacillus thuringiensis* var. *israelensis* and Dr. Julia Vorholt  
568 (ETH Zürich, Switzerland) for providing *At-LSPHERE* Leaf82 and helpful advice on this work.  
569 This work was funded by the DFG as part of the priority program DECryPT (to MS and ACV).

570

## 571 Supplementary Materials

572 **Supplementary Table S1** Primers used for RT-qPCR

573 **Supplementary Table S2** Amplicon sequence variants (ASVs) with a significantly different  
574 relative abundance in the phyllosphere microbiome of *Bti*- or WCS417-treated plants as  
575 compared to control-treated plants.

576 **Supplementary Figure S1** 16S rRNA gene amplicon sequencing results of the microbial  
577 standard control

578 **Supplementary Figure S2** Microbiome composition analysis of the phyllosphere of *A. thaliana*  
579 undergoing control and ISR-inducing treatments

580 **Supplementary Figure S3** Growth of ISR-inducing bacteria in *A. thaliana* leaves.

581 **Supplementary Figure S4** Systemic immunity in response to local leaf application of *Bti* and  
582 WCS417

583 **Supplementary Figure S5** WCS417 titers in Col-0 (wild type) and *npr1-1* mutant plants.

584

## 585 References

586 Bai, Y., Muller, D. B., Srinivas, G., Garrido-Oter, R., Potthoff, E., Rott, M., . . . Schulze-Lefert,  
587 P. (2015). Functional overlap of the *Arabidopsis* leaf and root microbiota. *Nature*,  
588 528(7582), 364-369. doi:10.1038/nature16192

589 Berendsen, R. L., Vismans, G., Yu, K., Song, Y., de Jonge, R., Burgman, W. P., . . . Pieterse,  
590 C. M. J. (2018). Disease-induced assemblage of a plant-beneficial bacterial  
591 consortium. *ISME J*, 12(6), 1496-1507. doi:10.1038/s41396-018-0093-1

592 Berg, G. (2009). Plant-microbe interactions promoting plant growth and health: perspectives  
593 for controlled use of microorganisms in agriculture. *Appl Microbiol Biotechnol*, 84(1),  
594 11-18. doi:10.1007/s00253-009-2092-7

595 Berger, S., Bell, E., & Mullet, J. E. (1996). Two Methyl Jasmonate-Insensitive Mutants Show  
596 Altered Expression of AtVsp in Response to Methyl Jasmonate and Wounding. *Plant*  
597 *Physiol*, 111(2), 525-531. doi:10.1104/pp.111.2.525

598 Bodenhausen, N., Horton, M. W., & Bergelson, J. (2013). Bacterial communities associated  
599 with the leaves and the roots of *Arabidopsis thaliana*. *PLoS One*, 8(2), e56329.  
600 doi:10.1371/journal.pone.0056329

601 Bravo, A., Gill, S. S., & Soberón, M. (2007). Mode of action of *Bacillus thuringiensis* Cry and  
602 Cyt toxins and their potential for insect control. *Toxicon : official journal of the*  
603 *International Society on Toxinology*, 49(4), 423-435. doi:10.1016/j.toxicon.2006.11.022

604 Breitenbach, H. H., Wenig, M., Wittek, F., Jorda, L., Maldonado-Alconada, A. M., Sarioglu, H.,  
605 . . . Vlot, A. C. (2014). Contrasting Roles of the Apoplastic Aspartyl Protease  
606 APOPLASTIC, ENHANCED DISEASE SUSCEPTIBILITY1-DEPENDENT1 and  
607 LEGUME LECTIN-LIKE PROTEIN1 in *Arabidopsis* Systemic Acquired Resistance.  
608 *Plant Physiol*, 165(2), 791-809. doi:10.1104/pp.114.239665

609 Bulgarelli, D., Rott, M., Schlaeppi, K., Ver Loren van Themaat, E., Ahmadinejad, N., Assenza,  
610 F., . . . Schulze-Lefert, P. (2012). Revealing structure and assembly cues for  
611 *Arabidopsis* root-inhabiting bacterial microbiota. *Nature*, 488, 91.  
612 doi:10.1038/nature11336

613 Callahan BJ, M. P., Rosen MJ, Han AW, Johnson AJA, Holmes SP. (2016). DADA2: High-  
614 resolution sample inference from Illumina amplicon data. *Nature Methods*.

615 Cao, H., Glazebrook, J., Clarke, J. D., Volko, S., & Dong, X. (1997). The *Arabidopsis* NPR1  
616 gene that controls systemic acquired resistance encodes a novel protein containing  
617 ankyrin repeats. *Cell*, 88(1), 57-63. doi:10.1016/s0092-8674(00)81858-9

618 Carlstrom, C. I., Field, C. M., Bortfeld-Miller, M., Muller, B., Sunagawa, S., & Vorholt, J. A.  
619 (2019). Synthetic microbiota reveal priority effects and keystone strains in the  
620 *Arabidopsis* phyllosphere. *Nat Ecol Evol*, 3(10), 1445-1454. doi:10.1038/s41559-019-  
621 0994-z

622 Cecchini, N. M., Roychoudhry, S., Speed, D. J., Steffes, K., Tambe, A., Zodrow, K., . . .  
623 Greenberg, J. T. (2019). Underground Azelaic Acid-Conferred Resistance to  
624 *Pseudomonas syringae* in *Arabidopsis*. *Mol Plant Microbe Interact*, 32(1), 86-94.  
625 doi:10.1094/MPMI-07-18-0185-R

626 Cecchini, N. M., Steffes, K., Schlappi, M. R., Gifford, A. N., & Greenberg, J. T. (2015).  
627       Arabidopsis AZI1 family proteins mediate signal mobilization for systemic defence  
628       priming. *Nat Commun*, 6, 7658. doi:10.1038/ncomms8658

629 Chaudhry, V., Runge, P., Sengupta, P., Doeblemann, G., Parker, J. E., & Kemen, E. (2020).  
630       Topic: Shaping the leaf microbiota: plant-microbe-microbe interactions. *J Exp Bot*.  
631       doi:10.1093/jxb/eraa417

632 Chelius, M. K., & Triplett, E. W. (2001). The Diversity of Archaea and Bacteria in Association  
633       with the Roots of *Zea mays* L. *Microb Ecol*, 41(3), 252-263.  
634       doi:10.1007/s002480000087

635 Chen, T., Nomura, K., Wang, X., Sohrabi, R., Xu, J., Yao, L., . . . He, S. Y. (2020). A plant  
636       genetic network for preventing dysbiosis in the phyllosphere. *Nature*, 580(7805), 653-  
637       657. doi:10.1038/s41586-020-2185-0

638 Chen, T., Nomura, K., Wang, X., Sohrabi, R., Xu, J., Yao, L., . . . He, S. Y. (2020). A plant  
639       genetic network for preventing dysbiosis in the phyllosphere. *Nature*, 580(7805), 653-  
640       657. doi:10.1038/s41586-020-2185-0

641 Chen, Y. C., Holmes, E. C., Rajniak, J., Kim, J. G., Tang, S., Fischer, C. R., . . . Sattely, E. S.  
642       (2018). N-hydroxy-pipecolic acid is a mobile metabolite that induces systemic disease  
643       resistance in *Arabidopsis*. *Proc Natl Acad Sci U S A*, 115(21), E4920-E4929.  
644       doi:10.1073/pnas.1805291115

645 Conrath, U., Beckers, G. J., Langenbach, C. J., & Jaskiewicz, M. R. (2015). Priming for  
646       enhanced defense. *Annu Rev Phytopathol*, 53, 97-119. doi:10.1146/annurev-phyto-  
647       080614-120132

648 Conrath, U., Beckers, G. J. M., Langenbach, C. J. G., & Jaskiewicz, M. R. (2015). Priming for  
649       Enhanced Defense. *Annu Rev Phytopathol*, 53(1), 97-119. doi:10.1146/annurev-phyto-  
650       080614-120132

651 Ding, P., Rekhter, D., Ding, Y., Feussner, K., Busta, L., Haroth, S., . . . Zhang, Y. (2016).  
652       Characterization of a Pipecolic Acid Biosynthesis Pathway Required for Systemic  
653       Acquired Resistance. *Plant Cell*, 28(10), 2603-2615. doi:10.1105/tpc.16.00486

654 Ding, Y., Sun, T., Ao, K., Peng, Y., Zhang, Y., Li, X., & Zhang, Y. (2018). Opposite Roles of  
655       Salicylic Acid Receptors NPR1 and NPR3/NPR4 in Transcriptional Regulation of Plant  
656       Immunity. *Cell*, 173(6), 1454-1467 e1415. doi:10.1016/j.cell.2018.03.044

657 Fu, Z. Q., Yan, S., Saleh, A., Wang, W., Ruble, J., Oka, N., . . . Dong, X. (2012). NPR3 and  
658       NPR4 are receptors for the immune signal salicylic acid in plants. *Nature*, 486(7402),  
659       228-232. doi:10.1038/nature11162

660 Goldberg, L. J. a. J. M. (1977). A bacterial spore demonstrating rapid larvicidal activity against  
661       Anopheles *sergentii*, *Uranotaenia unguiculata*, *Culex univittatus*, *Aedes aegypti* and  
662       *Culex pipiens*. *Mosquito News*, 37(3).

663 Gunasinghe, R. N., Ikiriwatte, C. J., & Karunaratne, A. M. (2004). The use of *Pantoea*  
664 *agglomerans* and *Flavobacterium* sp. to control banana pathogens. *The Journal of*  
665 *Horticultural Science and Biotechnology*, 79(6), 1002-1006.  
666 doi:10.1080/14620316.2004.11511852

667 Hartmann, M., Kim, D., Bernsdorff, F., Ajami-Rashidi, Z., Scholten, N., Schreiber, S., . . . Zeier,  
668 J. (2017). Biochemical Principles and Functional Aspects of Pipecolic Acid  
669 Biosynthesis in Plant Immunity. *Plant Physiol*, 174(1), 124-153.  
670 doi:10.1104/pp.17.00222

671 Hartmann, M., Zeier, T., Bernsdorff, F., Reichel-Deland, V., Kim, D., Hohmann, M., . . . Zeier,  
672 J. (2018). Flavin Monooxygenase-Generated N-Hydroxypipecolic Acid Is a Critical  
673 Element of Plant Systemic Immunity. *Cell*, 173(2), 456-469 e416.  
674 doi:10.1016/j.cell.2018.02.049

675 Hebbar, P., Berge, O., Heulin, T., & Singh, S. P. (1991). Bacterial antagonists of Sunflower  
676 (*Helianthus annuus* L.) fungal pathogens. *Plant and Soil*, 133(1), 131-140.  
677 doi:10.1007/BF00011907

678 Holmes, P. J. M. a. S. (2013). phyloseq: An R package for reproducible interactive analysis  
679 and graphics of microbiome census data. *PLoS One*, 8(4):e61217.

680 Hyakumachi, M., Nishimura, M., Arakawa, T., Asano, S., Yoshida, S., Tsushima, S., &  
681 Takahashi, H. (2013). *Bacillus thuringiensis* suppresses bacterial wilt disease caused  
682 by *Ralstonia solanacearum* with systemic induction of defense-related gene expression  
683 in tomato. *Microbes Environ*, 28(1), 128-134. doi:10.1264/jsme2.me12162

684 Ives, A. R., & Hughes, J. B. (2002). General relationships between species diversity and  
685 stability in competitive systems. *Am Nat*, 159(4), 388-395. doi:10.1086/338994

686 Jari Oksanen, F. G. B., Michael Friendly, Roeland Kindt, Pierre Legendre, Dan McGlinn, Peter  
687 R. Minchin, R. B. O'Hara, Gavin L. Simpson, Peter Solymos, M. Henry H. Stevens,  
688 Eduard Szoecs, Helene Wagner. (2019). vegan: Community Ecology Package.

689 Kim, S.-J., Moon, J.-Y., Weon, H.-Y., Ahn, J.-H., Chen, W.-M., & Kwon, S.-W. (2014).  
690 *Solimonas terrae* sp. nov., isolated from soil. *International Journal of Systematic and*  
691 *Evolutionary Microbiology*, 64(Pt\_4), 1218-1222.  
692 doi:<https://doi.org/10.1099/ijis.0.055574-0>

693 Kim, Y., Gilmour, S. J., Chao, L., Park, S., & Thomashow, M. F. (2020). *Arabidopsis* CAMTA  
694 Transcription Factors Regulate Pipecolic Acid Biosynthesis and Priming of Immunity  
695 Genes. *Mol Plant*, 13(1), 157-168. doi:10.1016/j.molp.2019.11.001

696 Kojima, H., Hossain, M. M., Kubota, M., & Hyakumachi, M. (2013). Involvement of the salicylic  
697 acid signaling pathway in the systemic resistance induced in *Arabidopsis* by plant  
698 growth-promoting fungus *Fusarium equiseti* GF19-1. *J Oleo Sci*, 62(6), 415-426.  
699 doi:10.5650/jos.62.415

700 Kolton, M., Sela, N., Elad, Y., & Cytryn, E. (2013). Comparative genomic analysis indicates  
701 that niche adaptation of terrestrial Flavobacteria is strongly linked to plant glycan  
702 metabolism. *PLoS One*, 8(9), e76704. doi:10.1371/journal.pone.0076704

703 Lim, G. H., Liu, H., Yu, K., Liu, R., Shine, M. B., Fernandez, J., . . . Kachroo, P. (2020). The  
704 plant cuticle regulates apoplastic transport of salicylic acid during systemic acquired  
705 resistance. *Sci Adv*, 6(19), eaaz0478. doi:10.1126/sciadv.aaz0478

706 Liu, Y., Sun, T., Sun, Y., Zhang, Y., Radojicic, A., Ding, Y., . . . Zhang, Y. (2020). Diverse Roles  
707 of the Salicylic Acid Receptors NPR1 and NPR3/NPR4 in Plant Immunity. *Plant Cell*,  
708 32(12), 4002-4016. doi:10.1105/tpc.20.00499

709 Love, M. I., Huber, W., Anders, S. (2014). Moderated estimation of fold change and dispersion  
710 for RNA-seq data with DESeq2. *Genome Biology*.

711 Lozupone, C., & Knight, R. (2005). UniFrac: a new phylogenetic method for comparing  
712 microbial communities. *Appl Environ Microbiol*, 71(12), 8228-8235.  
713 doi:10.1128/aem.71.12.8228-8235.2005

714 Lundberg, D. S., Lebeis, S. L., Paredes, S. H., Yourstone, S., Gehring, J., Malfatti, S., . . .  
715 Dangl, J. L. (2012). Defining the core *Arabidopsis thaliana* root microbiome. *Nature*,  
716 488(7409), 86-90. doi:10.1038/nature11237

717 Maimaiti, J., Zhang, Y., Yang, J., Cen, Y. P., Layzell, D. B., Peoples, M., & Dong, Z. (2007).  
718 Isolation and characterization of hydrogen-oxidizing bacteria induced following  
719 exposure of soil to hydrogen gas and their impact on plant growth. *Environ Microbiol*,  
720 9(2), 435-444. doi:10.1111/j.1462-2920.2006.01155.x

721 Martínez-Medina, A., Fernández, I., Sánchez-Guzmán, M. J., Jung, S. C., Pascual, J. A., &  
722 Pozo, M. J. (2013). Deciphering the hormonal signalling network behind the systemic  
723 resistance induced by *Trichoderma harzianum* in tomato. *Front Plant Sci*, 4, 206.  
724 doi:10.3389/fpls.2013.00206

725 Martínez-Medina, A., Flors, V., Heil, M., Mauch-Mani, B., Pieterse, C. M. J., Pozo, M. J., . . .  
726 Conrath, U. (2016). Recognizing Plant Defense Priming. *Trends Plant Sci*, 21(10), 818-  
727 822. doi:10.1016/j.tplants.2016.07.009

728 Mauch-Mani, B., Baccelli, I., Luna, E., & Flors, V. (2017). Defense Priming: An Adaptive Part  
729 of Induced Resistance. *Annu Rev Plant Biol*, 68, 485-512. doi:10.1146/annurev-  
730 arplant-042916-041132

731 McMurdie, P. J., & Holmes, S. (2014). Waste Not, Want Not: Why Rarefying Microbiome Data  
732 Is Inadmissible. *PLOS Computational Biology*, 10(4), e1003531.  
733 doi:10.1371/journal.pcbi.1003531

734 Navarova, H., Bernsdorff, F., Doring, A. C., & Zeier, J. (2012). Pipecolic acid, an endogenous  
735 mediator of defense amplification and priming, is a critical regulator of inducible plant  
736 immunity. *Plant Cell*, 24(12), 5123-5141. doi:10.1105/tpc.112.103564

737 Nguyen, N. H., Trotel-Aziz, P., Villaume, S., Rabenoelina, F., Schwarzenberg, A., Nguema-  
738 Ona, E., . . . Aziz, A. (2020). *Bacillus subtilis* and *Pseudomonas fluorescens* Trigger  
739 Common and Distinct Systemic Immune Responses in *Arabidopsis thaliana* Depending  
740 on the Pathogen Lifestyle. *Vaccines (Basel)*, 8(3). doi:10.3390/vaccines8030503

741 Nickstadt, A. T., Bart. Feussner, Ivo. Kangasjärvi, Jaakko. Zeier, Jürgen. Loeffler, Christiane.  
742 Scheel, Dierk. Berger, Susanne. (2004). The jasmonate-insensitive mutant *jin1* shows  
743 increased resistance to biotrophic as well as necrotrophic pathogens. *Molecular Plant  
744 Pathology*, 5(5), 425-434. doi:<https://doi.org/10.1111/j.1364-3703.2004.00242.x>

745 Nie, P., Li, X., Wang, S., Guo, J., Zhao, H., & Niu, D. (2017). Induced Systemic Resistance  
746 against *Botrytis cinerea* by *Bacillus cereus* AR156 through a JA/ET- and NPR1-  
747 Dependent Signaling Pathway and Activates PAMP-Triggered Immunity in  
748 *Arabidopsis*. *Front Plant Sci*, 8, 238. doi:10.3389/fpls.2017.00238

749 Niu, D. D., Liu, H. X., Jiang, C. H., Wang, Y. P., Wang, Q. Y., Jin, H. L., & Guo, J. H. (2011).  
750 The plant growth-promoting rhizobacterium *Bacillus cereus* AR156 induces systemic  
751 resistance in *Arabidopsis thaliana* by simultaneously activating salicylate- and  
752 jasmonate/ethylene-dependent signaling pathways. *Mol Plant Microbe Interact*, 24(5),  
753 533-542. doi:10.1094/mpmi-09-10-0213

754 Park, S. W., Kaimoyo, E., Kumar, D., Mosher, S., & Klessig, D. F. (2007). Methyl salicylate is  
755 a critical mobile signal for plant systemic acquired resistance. *Science*, 318(5847), 113-  
756 116. doi:10.1126/science.1147113

757 Peterson, S. B., Dunn, A. K., Klimowicz, A. K., & Handelsman, J. (2006). Peptidoglycan from  
758 *Bacillus cereus* mediates commensalism with rhizosphere bacteria from the  
759 Cytophaga-Flavobacterium group. *Appl Environ Microbiol*, 72(8), 5421-5427.  
760 doi:10.1128/aem.02928-05

761 Pieterse, C. M., Van der Does, D., Zamioudis, C., Leon-Reyes, A., & Van Wees, S. C. (2012).  
762 Hormonal modulation of plant immunity. *Annu Rev Cell Dev Biol*, 28, 489-521.  
763 doi:10.1146/annurev-cellbio-092910-154055

764 Pieterse, C. M., van Wees, S. C., Hoffland, E., van Pelt, J. A., & van Loon, L. C. (1996).  
765 Systemic resistance in *Arabidopsis* induced by biocontrol bacteria is independent of  
766 salicylic acid accumulation and pathogenesis-related gene expression. *Plant Cell*, 8(8),  
767 1225-1237. doi:10.1105/tpc.8.8.1225

768 Pieterse, C. M., van Wees, S. C., van Pelt, J. A., Knoester, M., Laan, R., Gerrits, H., . . . van  
769 Loon, L. C. (1998). A novel signaling pathway controlling induced systemic resistance  
770 in *Arabidopsis*. *Plant Cell*, 10(9), 1571-1580. doi:10.1105/tpc.10.9.1571

771 Pieterse, C. M., Zamioudis, C., Berendsen, R. L., Weller, D. M., Van Wees, S. C., & Bakker,  
772 P. A. (2014). Induced systemic resistance by beneficial microbes. *Annu Rev  
773 Phytopathol*, 52, 347-375. doi:10.1146/annurev-phyto-082712-102340

774 Pozo, M. J., Van Der Ent, S., Van Loon, L. C., & Pieterse, C. M. (2008). Transcription factor  
775 MYC2 is involved in priming for enhanced defense during rhizobacteria-induced  
776 systemic resistance in *Arabidopsis thaliana*. *New Phytol*, 180(2), 511-523.  
777 doi:10.1111/j.1469-8137.2008.02578.x

778 R Development Core Team. (2020). R: A language and environment for statistical computing.  
779 *R Foundation for Statistical Computing, Vienna*.

780 Raddadi, N., Cherif, A., Ouzari, H., Marzorati, M., Brusetti, L., Boudabous, A., & Daffonchio,  
781 D. (2007). *Bacillus thuringiensis* beyond insect biocontrol: plant growth promotion and  
782 biosafety of polyvalent strains. *Annals of Microbiology*, 57(4), 481-494.  
783 doi:10.1007/bf03175344

784 Rekhter, D., Lüdke, D., Ding, Y., Feussner, K., Zienkiewicz, K., Lipka, V., . . . Feussner, I.  
785 (2019). Isochorismate-derived biosynthesis of the plant stress hormone salicylic acid.  
786 *Science*, 365(6452), 498-502. doi:10.1126/science.aaw1720

787 Riedlmeier, M., Ghirardo, A., Wenig, M., Knappe, C., Koch, K., Georgii, E., . . . Vlot, A. C.  
788 (2017). Monoterpene Support Systemic Acquired Resistance within and between  
789 Plants. *Plant Cell*, 29(6), 1440-1459. doi:10.1105/tpc.16.00898

790 Rudrappa, T., Czymbek, K. J., Pare, P. W., & Bais, H. P. (2008). Root-secreted malic acid  
791 recruits beneficial soil bacteria. *Plant Physiol*, 148(3), 1547-1556.  
792 doi:10.1104/pp.108.127613

793 Sang, M. K., & Kim, K. D. (2012). The volatile-producing *Flavobacterium johnsoniae* strain  
794 GSE09 shows biocontrol activity against *Phytophthora capsici* in pepper. *J Appl*  
795 *Microbiol*, 113(2), 383-398. doi:10.1111/j.1365-2672.2012.05330.x

796 Schlaeppi, K., & Bulgarelli, D. (2015). The plant microbiome at work. *Mol Plant Microbe*  
797 *Interact*, 28(3), 212-217. doi:10.1094/mpmi-10-14-0334-fi

798 Schliep, K., Potts, A. J., Morrison, D. A., & Grimm, G. W. (2017). Intertwining phylogenetic  
799 trees and networks. *Methods in Ecology and Evolution*, 8(10), 1212-1220.  
800 doi:<https://doi.org/10.1111/2041-210X.12760>

801 Shine, M. B., Gao, Q. M., Chowda-Reddy, R. V., Singh, A. K., Kachroo, P., & Kachroo, A.  
802 (2019). Glycerol-3-phosphate mediates rhizobia-induced systemic signaling in  
803 soybean. *Nat Commun*, 10(1), 5303. doi:10.1038/s41467-019-13318-8

804 Simpson, E. H. (1949). Measurement of Diversity. *Nature*, 163(4148), 688-688.  
805 doi:10.1038/163688a0

806 Song, J. T., Lu, H., McDowell, J. M., & Greenberg, J. T. (2004). A key role for ALD1 in activation  
807 of local and systemic defenses in *Arabidopsis*. *Plant J*, 40(2), 200-212.  
808 doi:10.1111/j.1365-313X.2004.02200.x

809 Spellerberg, I. F., & Fedor, P. J. (2003). A tribute to Claude Shannon (1916–2001) and a plea  
810 for more rigorous use of species richness, species diversity and the ‘Shannon–Wiener’

811 Index. *Global Ecology and Biogeography*, 12(3), 177-179.  
812 doi:<https://doi.org/10.1046/j.1466-822X.2003.00015.x>

813 Sun, T., Huang, J., Xu, Y., Verma, V., Jing, B., Sun, Y., . . . Li, X. (2020). Redundant CAMTA  
814 Transcription Factors Negatively Regulate the Biosynthesis of Salicylic Acid and N-  
815 Hydroxypipelicolic Acid by Modulating the Expression of SARD1 and CBP60g. *Mol  
816 Plant*, 13(1), 144-156. doi:10.1016/j.molp.2019.10.016

817 Takahashi, H., Nakaho, K., Ishihara, T., Ando, S., Wada, T., Kanayama, Y., . . . Hyakumachi,  
818 M. (2014). Transcriptional profile of tomato roots exhibiting *Bacillus thuringiensis*-  
819 induced resistance to *Ralstonia solanacearum*. *Plant Cell Reports*, 33(1), 99-110.  
820 doi:10.1007/s00299-013-1515-1

821 Tamošiūnė, I., Gelvonauskienė, D., Ragauskaitė, L., Koga, K., Shiratani, M., & Baniulis, D.  
822 (2020). Cold plasma treatment of *Arabidopsis thaliana* (L.) seeds modulates plant-  
823 associated microbiome composition. *Applied Physics Express*, 13. doi:10.35848/1882-  
824 0786/ab9712

825 Teixeira, P. J. P., Colaianni, N. R., Fitzpatrick, C. R., & Dangl, J. L. (2019). Beyond pathogens:  
826 microbiota interactions with the plant immune system. *Curr Opin Microbiol*, 49, 7-17.  
827 doi:10.1016/j.mib.2019.08.003

828 Ton, J., Van Pelt, J. A., Van Loon, L. C., & Pieterse, C. M. (2002). Differential effectiveness of  
829 salicylate-dependent and jasmonate/ethylene-dependent induced resistance in  
830 *Arabidopsis*. *Mol Plant Microbe Interact*, 15(1), 27-34. doi:10.1094/MPMI.2002.15.1.27

831 van de Mortel, J. E., de Vos, R. C. H., Dekkers, E., Pineda, A., Guillod, L., Bouwmeester, K., .  
832 . . . Raaijmakers, J. M. (2012). Metabolic and Transcriptomic Changes Induced in  
833 *Arabidopsis* by the Rhizobacterium *Pseudomonas fluorescens* SS101. *Plant  
834 Physiology*, 160(4), 2173-2188. doi:10.1104/pp.112.207324

835 Van der Ent, S., Verhagen, B. W., Van Doorn, R., Bakker, D., Verlaan, M. G., Pel, M. J., . . .  
836 Pieterse, C. M. (2008). MYB72 is required in early signaling steps of rhizobacteria-  
837 induced systemic resistance in *Arabidopsis*. *Plant Physiol*, 146(3), 1293-1304.  
838 doi:10.1104/pp.107.113829

839 van Loon, L. C., Rep, M., & Pieterse, C. M. (2006). Significance of inducible defense-related  
840 proteins in infected plants. *Annu Rev Phytopathol*, 44, 135-162.  
841 doi:10.1146/annurev.phyto.44.070505.143425

842 Vlot, A. C., Dempsey, D. A., & Klessig, D. F. (2009). Salicylic Acid, a multifaceted hormone to  
843 combat disease. *Annu Rev Phytopathol*, 47, 177-206.  
844 doi:10.1146/annurev.phyto.050908.135202

845 Vlot, A. C., Sales, J. H., Lenk, M., Bauer, K., Brambilla, A., Sommer, A., . . . Nayem, S. (2020).  
846 Systemic propagation of immunity in plants. *New Phytol*. doi:10.1111/nph.16953

847 Vogel, C., Bodenhausen, N., Gruisse, W., & Vorholt, J. A. (2016). The *Arabidopsis* leaf  
848 transcriptome reveals distinct but also overlapping responses to colonization by  
849 phyllosphere commensals and pathogen infection with impact on plant health. *New*  
850 *Phytol*, 212(1), 192-207. doi:10.1111/nph.14036

851 Vorholt, J. A. (2012). Microbial life in the phyllosphere. *Nature Reviews Microbiology*, 10, 828.  
852 doi:10.1038/nrmicro2910

853 Waller, F., Achatz, B., Baltruschat, H., Fodor, J., Becker, K., Fischer, M., . . . Kogel, K. H.  
854 (2005). The endophytic fungus *Piriformospora indica* reprograms barley to salt-stress  
855 tolerance, disease resistance, and higher yield. *Proc Natl Acad Sci U S A*, 102(38),  
856 13386-13391. doi:10.1073/pnas.0504423102

857 Wang, C., Liu, R., Lim, G. H., de Lorenzo, L., Yu, K., Zhang, K., . . . Kachroo, P. (2018).  
858 Pipecolic acid confers systemic immunity by regulating free radicals. *Sci Adv*, 4(5),  
859 eaar4509. doi:10.1126/sciadv.aar4509

860 Wenig, M., Ghirardo, A., Sales, J. H., Pabst, E. S., Breitenbach, H. H., Antritter, F., . . . Vlot, A.  
861 C. (2019). Systemic acquired resistance networks amplify airborne defense cues. *Nat*  
862 *Commun*, 10(1), 3813. doi:10.1038/s41467-019-11798-2

863 Wildermuth, M. C., Dewdney, J., Wu, G., & Ausubel, F. M. (2001). Isochorismate synthase is  
864 required to synthesize salicylic acid for plant defence. *Nature*, 414(6863), 562-565.  
865 doi:10.1038/35107108

866 Wright, E. S. (2016). Using DECIIPHER v2.0 to Analyze Big Biological Sequence Data in R.  
867 *The R Journal*, 8, 352-359. doi:10.32614/RJ-2016-025

868 Wu, L., Huang, Z., Li, X., Ma, L., Gu, Q., Wu, H., . . . Gao, X. (2018). Stomatal Closure and  
869 SA-, JA/ET-Signaling Pathways Are Essential for *Bacillus amyloliquefaciens* FZB42 to  
870 Restrict Leaf Disease Caused by *Phytophthora nicotianae* in *Nicotiana benthamiana*.  
871 *Front Microbiol*, 9, 847. doi:10.3389/fmicb.2018.00847

872 Yilmaz, P., Parfrey, L. W., Yarza, P., Gerken, J., Pruesse, E., Quast, C., . . . Glöckner, F. O.  
873 (2013). The SILVA and “All-species Living Tree Project (LTP)” taxonomic frameworks.  
874 *Nucleic Acids Research*, 42(D1), D643-D648. doi:10.1093/nar/gkt1209

875 Yu, K., Pieterse, C. M. J., Bakker, P., & Berendsen, R. L. (2019). Beneficial microbes going  
876 underground of root immunity. *Plant Cell Environ*, 42(10), 2860-2870.  
877 doi:10.1111/pce.13632

878

879

880 **Figure legends**

881

882 **Figure 1.** *Bacillus thuringiensis* var. *israelensis* (*Bti*) and *Pseudomonas simiae* WCS417r  
883 (WCS417) trigger induced systemic resistance (ISR) in *Arabidopsis thaliana* in the absence of  
884 SA and JA marker gene expression or priming. The roots of 10-day-old, sterile-grown *A.*  
885 *thaliana* seedlings were inoculated with *Bti* (blue bars), WCS417 (green bars), or a  
886 corresponding control solution (yellow bars). Following 3.5 weeks on soil, the leaves of the  
887 treated plants were infiltrated with *P. syringae* pathovar *tomato* (*Pst*). **(A)** *In planta* *Pst* titers at  
888 4dpi. Bars represent the mean of three biologically independent experiments, including three  
889 replicates each  $\pm$  SD. Asterisks indicate significant differences between the treatments  
890 indicated by the corresponding lines (pairwise Wilcoxon test, adjusted for multiple testing by  
891 Benjamini-Hochberg procedure, \*\*\*\*,  $p < 0.0001$ ; ns, not significantly different). **(B)** *PDF1.2*,  
892 *VSP2*, and *PR1* transcript accumulation in leaves of plants treated as in (A) and sampled  
893 before infection (upper panel) or 6 hours (h) after inoculation of the leaves with *Pst* (lower  
894 panel). Transcript accumulation was determined relative to that of *UBI/QUITIN* by RT-qPCR.  
895 Bars represent mean values of three biologically independent experiments  $\pm$  SD. Statistically  
896 significant differences were excluded using pairwise Wilcoxon test, adjusted for multiple testing  
897 by Benjamini-Hochberg procedure.

898

899 **Figure 2.** Characterization of the molecular requirements of *Bti*- and WCS417-triggered ISR.  
900 The roots of 10-day-old seedlings of the genotypes indicated above the panels were inoculated  
901 with *Bti* (blue bars), WCS417 (green bars), or a corresponding control solution (yellow bars).  
902 Following 3.5 weeks on soil, the leaves of the plants were inoculated with *Pst*. The resulting *in*  
903 *planta* *Pst* titers at 4 dpi are shown. Bars represent the mean of three biologically independent  
904 experiments, including three replicates each  $\pm$  SD. Asterisks indicate significant differences  
905 between the treatments indicated by the corresponding lines (pairwise Wilcoxon test, adjusted  
906 for multiple testing by Benjamini-Hochberg procedure, \*,  $p < 0.05$ , \*\*,  $p < 0.01$ , \*\*\*,  $p < 0.001$ ,  
907 \*\*\*\*,  $p < 0.0001$ ; ns, not significantly different).

908

909 **Figure 3.** Distribution of 16S rRNA gene amplicon reads among the ten most abundant phyla  
910 in the *A. thaliana* phyllosphere microbiome of plants undergoing control (in yellow) and ISR-  
911 inducing treatments with *Bti* (in blue) or WCS417 (in green). Circle sizes represent mean read  
912 counts from five (*Bti* and WCS417) to six (control) biologically independent replicate  
913 experiments.

914

915 **Figure 4.** Diversity analysis of the phyllosphere microbiome of *A. thaliana* undergoing control  
916 (in yellow) and ISR-inducing treatments with *Bti* (in blue) or WCS417 (in green). **(A)** Rarefaction

917 curves of the sequenced samples correlating the number of detected amplicon sequence  
918 variants (ASVs) on the Y-axis to the number of sequenced reads on the X-axis. Samples from  
919 WCS417-treated plants contain significantly fewer ASVs (pairwise Wilcoxon test, adjusted for  
920 multiple testing by Benjamini-Hochberg procedure, WCS417 – control,  $p = 0.013$ ). **(B)**  
921 Shannon's Index (left) and Simpson's Index (right). The Y-axis represents the respective index  
922 value, and dots indicate the values of individual samples. Samples from WCS417-treated  
923 plants have a lower Shannon's Index than *Bti*- or control-treated plants (pairwise Wilcoxon test,  
924 adjusted for multiple testing by Benjamini-Hochberg procedure, WCS417 – control, Shannon:  
925  $p = 0.013$ , Simpson:  $p = 0.38$ ).

926

927 **Figure 5.** Abundance of distinct bacterial species in the phyllosphere microbiome of *A. thaliana*  
928 undergoing control (in yellow) and ISR-inducing treatments with *Bti* (in blue) or WCS417 (in  
929 green). Boxplots indicate average numbers of sequenced reads corresponding to the species  
930 indicated above the panels from five (*Bti* and WCS417) to six (control) samples after  
931 normalization to total read counts per sample. Asterisks indicate significant differences  
932 between the treatments indicated by the corresponding lines (pairwise Wilcoxon test, adjusted  
933 for multiple testing by Benjamini-Hochberg procedure, \*,  $p < 0.05$ , \*\*,  $p < 0.01$ , \*\*\*,  $p < 0.001$ ).

934

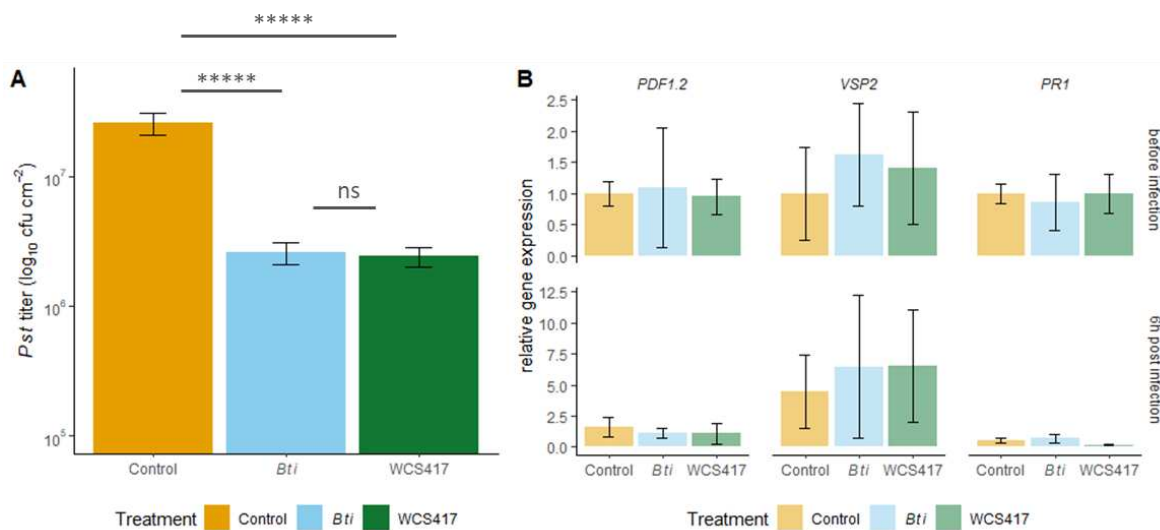
935 **Figure 6.** Local plant-microbe-microbe interactions. Leaves of 4-5-week-old Col-0 wild type  
936 and *npr1* mutant plants (as indicated above the panels) were infiltrated with WCS417 (green  
937 bars in A/C), *At-L-Sphere Flavobakterium sp.* Leaf82 (L82; purple bars in B), or a  
938 corresponding control solution (yellow bars in A-C). Two days later, the same leaves were  
939 infiltrated with *Pst* (A/B) or Leaf82 (C), titers of which were determined at 4 dpi. Bars represent  
940 average *in planta* *Pst* (A/B) and Leaf82 (C) titers from 6 to 9 samples derived from two (C) to  
941 three (A/B) biologically independent experiments  $\pm$  SD. Asterisks indicate significant  
942 differences between the treatments indicated by the corresponding lines (pairwise Wilcoxon  
943 test, adjusted for multiple testing by Benjamini-Hochberg procedure, \*,  $p < 0.05$ , \*\*,  $p < 0.01$ ;  
944 ns, not significantly different).

945

946

947

948  
949  
950

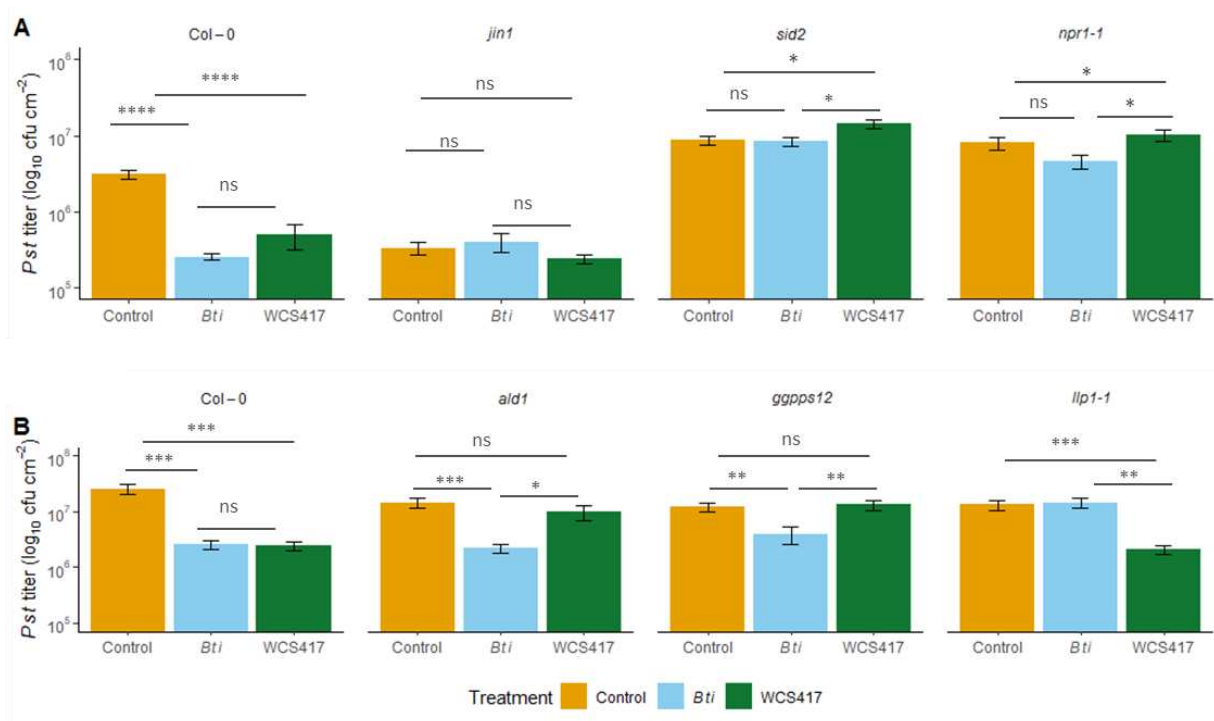


951  
952

953 **Figure 1.** *Bacillus thuringiensis* var. *israelensis* (*Bti*) and *Pseudomonas simiae* WCS417r  
954 trigger induced systemic resistance (ISR) in *Arabidopsis thaliana* in the absence of  
955 SA and JA marker gene expression or priming. The roots of 10-day-old, sterile-grown *A.*  
956 *thaliana* seedlings were inoculated with *Bti* (blue bars), WCS417 (green bars), or a  
957 corresponding control solution (yellow bars). Following 3.5 weeks on soil, the leaves of the  
958 treated plants were infiltrated with *P. syringae* pathovar *tomato* (*Pst*). **(A)** *In planta* *Pst* titers at  
959 4dpi. Bars represent the mean of three biologically independent experiments, including three  
960 replicates each  $\pm$  SD. Asterisks indicate significant differences between the treatments  
961 indicated by the corresponding lines (pairwise Wilcoxon test, adjusted for multiple testing by  
962 Benjamini-Hochberg procedure, \*\*\*\*,  $p < 0.0001$ ; ns, not significantly different). **(B)** *PDF1.2*,  
963 *VSP2*, and *PR1* transcript accumulation in leaves of plants treated as in (A) and sampled  
964 before infection (upper panel) or 6 hours (h) after inoculation of the leaves with *Pst* (lower  
965 panel). Transcript accumulation was determined relative to that of *UBIQUITIN* by RT-qPCR.  
966 Bars represent mean values of three biologically independent experiments  $\pm$  SD. Statistically  
967 significant differences were excluded using pairwise Wilcoxon test, adjusted for multiple testing  
968 by Benjamini-Hochberg procedure.

969

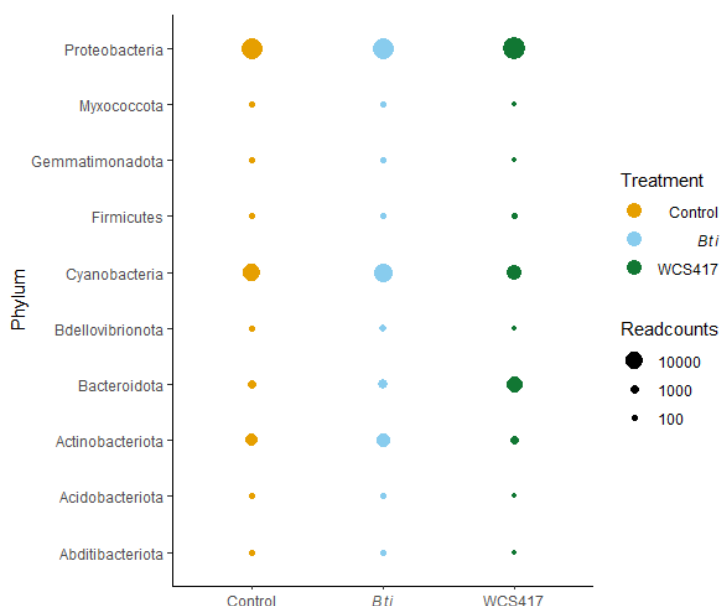
970  
971  
972  
973



974  
975

976 **Figure 2.** Characterization of the molecular requirements of *Bti*- and WCS417-triggered ISR.  
977 The roots of 10-day-old seedlings of the genotypes indicated above the panels were inoculated  
978 with *Bti* (blue bars), WCS417 (green bars), or a corresponding control solution (yellow bars).  
979 Following 3.5 weeks on soil, the leaves of the plants were inoculated with *Pst*. The resulting *in*  
980 *planta* *Pst* titers at 4 dpi are shown. Bars represent the mean of three biologically independent  
981 experiments, including three replicates each  $\pm$  SD. Asterisks indicate significant differences  
982 between the treatments indicated by the corresponding lines (pairwise Wilcoxon test, adjusted  
983 for multiple testing by Benjamini-Hochberg procedure, \*,  $p < 0.05$ , \*\*,  $p < 0.01$ , \*\*\*,  $p < 0.001$ ,  
984 \*\*\*\*,  $p < 0.0001$ ; ns, not significantly different).

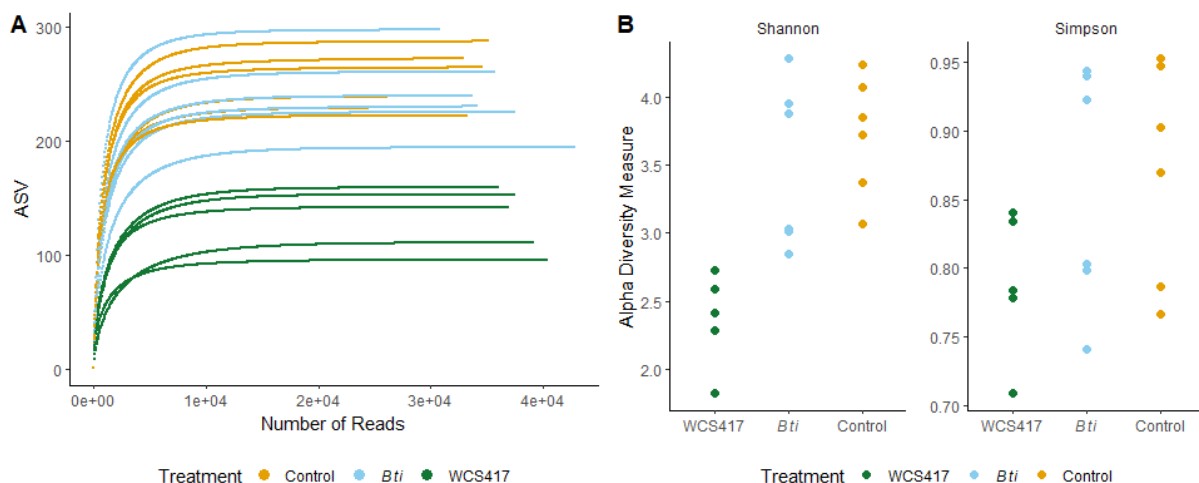
985  
986  
987  
988



989  
990  
991 **Figure 3.** Distribution of 16S rRNA gene amplicon reads among the ten most abundant phyla  
992 in the *A. thaliana* phyllosphere microbiome of plants undergoing control (in yellow) and ISR-  
993 inducing treatments with *Bti* (in blue) or WCS417 (in green). Circle sizes represent mean read  
994 counts from five (*Bti* and WCS417) to six (control) biologically independent replicate  
995 experiments.

996  
997

998  
999  
1000  
1001

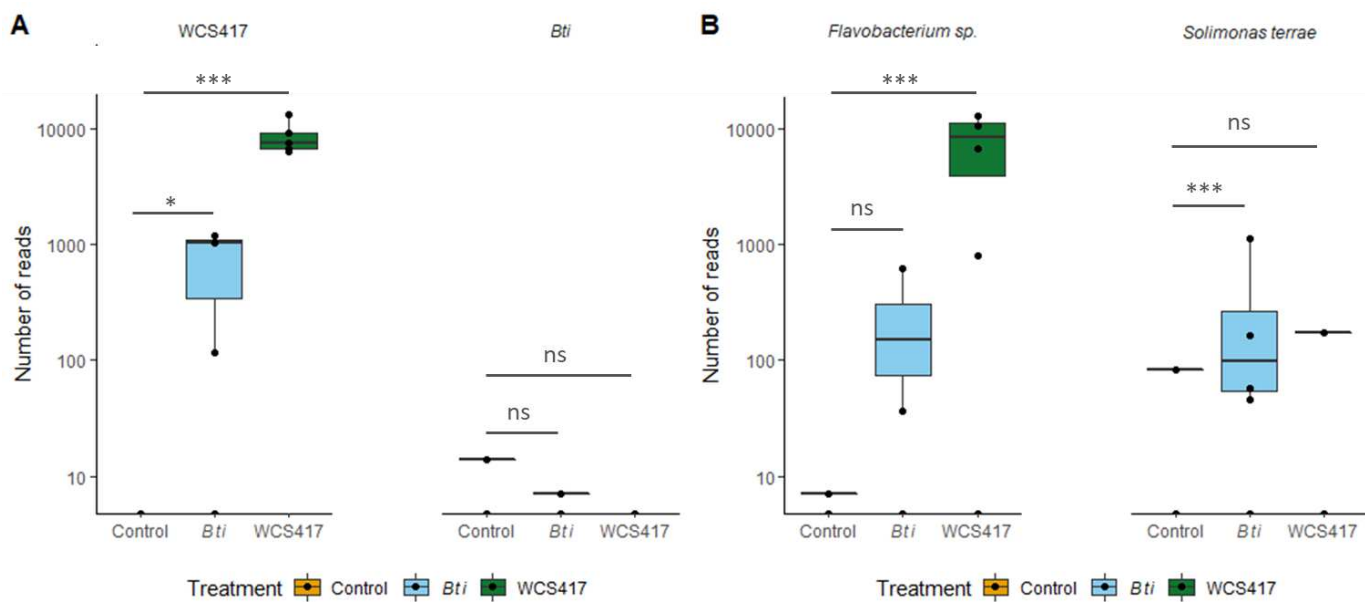


1002  
1003

1004 **Figure 4.** Diversity analysis of the phyllosphere microbiome of *A. thaliana* undergoing control  
1005 (in yellow) and ISR-inducing treatments with *Bti* (in blue) or WCS417 (in green). **(A)** Rarefaction  
1006 curves of the sequenced samples correlating the number of detected amplicon sequence  
1007 variants (ASVs) on the Y-axis to the number of sequenced reads on the X-axis. Samples from  
1008 WCS417-treated plants contain significantly fewer ASVs (pairwise Wilcoxon test, adjusted for  
1009 multiple testing by Benjamini-Hochberg procedure, WCS417 – control,  $p = 0.013$ ). **(B)**  
1010 Shannon's Index (left) and Simpson's Index (right). The Y-axis represents the respective index  
1011 value, and dots indicate the values of individual samples. Samples from WCS417-treated  
1012 plants have a lower Shannon's Index than *Bti*- or control-treated plants (pairwise Wilcoxon test,  
1013 adjusted for multiple testing by Benjamini-Hochberg procedure, WCS417 – control, Shannon:  
1014  $p = 0.013$ , Simpson:  $p = 0.38$ ).

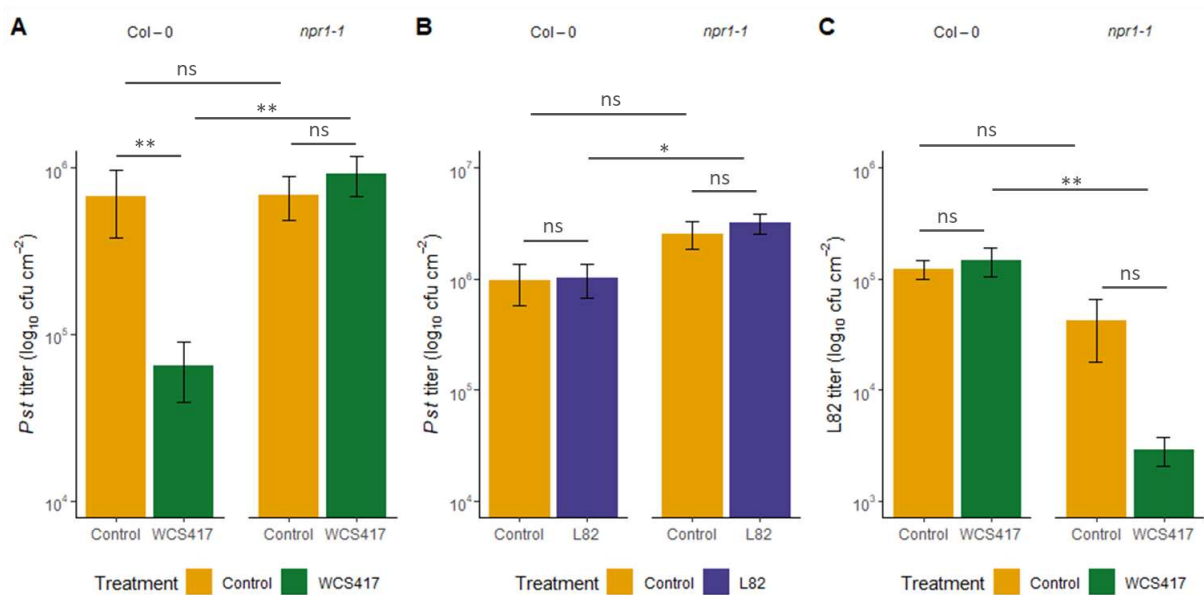
1015

1016  
1017  
1018  
1019



1020  
1021  
1022  
1023 **Figure 5.** Abundance of distinct bacterial species in the phyllosphere microbiome of *A. thaliana*  
1024 undergoing control (in yellow) and ISR-inducing treatments with *Bti* (in blue) or WCS417 (in  
1025 green). Boxplots indicate average numbers of sequenced reads corresponding to the species  
1026 indicated above the panels from five (*Bti* and WCS417) to six (control) samples after  
1027 normalization to total read counts per sample. Asterisks indicate significant differences  
1028 between the treatments indicated by the corresponding lines (pairwise Wilcoxon test, adjusted  
1029 for multiple testing by Benjamini-Hochberg procedure, \*,  $p < 0.05$ , \*\*,  $p < 0.01$ , \*\*\*,  $p < 0.001$ ).  
1030  
1031  
1032  
1033  
1034

1035  
1036  
1037  
1038



1039  
1040  
1041 **Figure 6.** Local plant-microbe-microbe interactions. Leaves of 4-5-week-old Col-0 wild type  
1042 and *npr1* mutant plants (as indicated above the panels) were infiltrated with WCS417 (green  
1043 bars in A/C), At-L-Sphere *Flavobakterium* sp. Leaf82 (L82; purple bars in B), or a  
1044 corresponding control solution (yellow bars in A-C). Two days later, the same leaves were  
1045 infiltrated with *Pst* (A/B) or Leaf82 (C), titers of which were determined at 4 dpi. Bars represent  
1046 average *in planta* *Pst* (A/B) and Leaf82 (C) titers from 6 to 9 samples derived from two (C) to  
1047 three (A/B) biologically independent experiments  $\pm$  SD. Asterisks indicate significant  
1048 differences between the treatments indicated by the corresponding lines (pairwise Wilcoxon  
1049 test, adjusted for multiple testing by Benjamini-Hochberg procedure, \*,  $p < 0.05$ , \*\*,  $p < 0.01$ ;  
1050 ns, not significantly different).

1051